UNIVERSIDADE ESTADUAL DE CAMPINAS
INSTITUTO DE GEOCIÊNCIAS

TITO AURELIANO NETO

A EVOLUÇÃO DO SISTEMA RESPIRATÓRIO DE DINOSSAUROS SOB A PERSPECTIVA DA PALEOHISTOLOGIA

THE EVOLUTION OF THE DINOSAUR RESPIRATORY SYSTEM FROM THE PALEOHISTOLOGY PERSPECTIVE

CAMPINAS

2023

TITO AURELIANO NETO

A EVOLUÇÃO DO SISTEMA RESPIRATÓRIO DE DINOSSAUROS SOB A PERSPECTIVA DA PALEOHISTOLOGIA

THE EVOLUTION OF THE DINOSAUR RESPIRATORY SYSTEM FROM THE PALEOHISTOLOGY PERSPECTIVE

TESE APRESENTADA AO INSTITUTO DE GEOCIÊNCIAS DA UNIVERSIDADE ESTADUAL DE CAMPINAS PARA OBTENÇÃO DO TÍTULO DE DOUTOR EM CIÊNCIAS NA ÁREA DE GEOLOGIA E RECURSOS NATURAIS

THESIS PRESENTED TO THE INSTITUTE OF GEOSCIENCES OF THE UNIVERSITY OF CAMPINAS TO OBTAIN THE DEGREE OF DOCTOR IN SCIENCES IN AREA OF GEOLOGY AND NATURAL RESOURCES

Orientadora: FRESIA SOLEDAD TORRES RICARDI BRANCO
Co-orientador: MARCELO ADORNA FERNANDES

ESTE EXEMPLAR CORRESPONDE À VERSÃO FINAL DA TESE DEFENDIDA PELO ESTUDANTE TITO AURELIANO NETO, E ORIENTADA PELA PROFA. DRA. FRESIA SOLEDAD TORRES RICARDI BRANCO E CO-ORIENTADA PELA PROF. MARCELO ADORNA FERNANDES

CAMPINAS

2023

Ficha catalográfica
Universidade Estadual de Campinas
Biblioteca do Instituto de Geociências
Marta dos Santos - CRB 8/5892

Aureliano Neto, Tito, 1989-
Au64e The evolution of the dinosaur respiratory system from the paleohistology perspective / Tito Aureliano Neto. – Campinas, SP : [s.n.], 2023.

Orientador: Fresia Soledad Ricardi Torres Branco.
Coorientador: Marcelo Adorna Fernandes.
Tese (doutorado) – Universidade Estadual de Campinas, Instituto de Geociências.

1. Histologia. 2. Petrologia. 3. Mineralogia. 4. Anatomia. 5. Paleontologia. I. Ricardi-Branco, Fresia, 1963-. II. Fernandes, Marcelo Adorna. III. Universidade Estadual de Campinas. Instituto de Geociências. IV. Título.

Informações Complementares

Título em outro idioma: A evolução do sistema respiratório de dinossauros sob a perspectiva da paleohistologia
Palavras-chave em inglês:
Histology
Petrology
Mineralogy
Anatomy
Paleontology
Área de concentração: Geologia e Recursos Naturais
Titulação: Doutor em Ciências
Banca examinadora:
Fresia Soledad Ricardi Torres Branco [Orientador]
Pedro Victor Buck
Giorgio Basilici
Felipe Lima Pinheiro
Ariel Milani Martine
Data de defesa: 24-02-2023
Programa de Pós-Graduação: Geociências

Identificação e informações acadêmicas do(a) aluno(a)
- ORCID do autor: https://orcid.org/0000-0002-6918-0519
- Currículo Lattes do autor: http://buscatextual.cnpq.br/buscatextual/visu

UNIVERSIDADE ESTADUAL DE CAMPINAS
INSTITUTO DE GEOCIÊNCIAS

AUTOR: Tito Aureliano Neto

A EVOLUÇÃO DO SISTEMA RESPIRATÓRIO DE DINOSSAUROS SOB A PERSPECTIVA DA PALEOHISTOLOGIA

THE EVOLUTION OF THE DINOSAUR RESPIRATORY SYSTEM FROM THE PALEOHISTOLOGY PERSPECTIVE

ORIENTADORA: Profa. Dra. Fresia Soledad Torres Ricardi Branco

COORIENTADOR: Prof. Dr. Marcelo Adorna Fernandes

Aprovado em: 24/02/2023

EXAMINADORES:

Profa. Dra. Fresia Soledad Torres Ricardi Branco – Presidente

Prof. Dr. Ariel Milani Martine

Prof. Dr. Felipe Lima Pinheiro

Prof. Dr. Giorgio Basilici

Prof. Dr. Pedro Victor Buck

A Ata de Defesa assinada pelos membros da Comissão Examinadora consta no processo de vida acadêmica do estudante.

Campinas, 24 de fevereiro de 2023.

SÚMULA CURRICULAR

Tito Aureliano Neto

Tito Aureliano é graduado em Geologia pela UFPE, e Mestre e Doutor em Ciências pela Unicamp. Tem mais de 15 anos de experiência em PALEONTOLOGIA, ESTRATIGRAFIA e PETROLOGIA SEDIMENTAR. Sua especialização está no estudo de tecidos biomineralizados: a PALEOHISTOLOGIA. Também possui *expertise* em MORFOLOGIA, PALEOPATOLOGIA e PALEOPARASITOLOGIA. Possui dezenas de publicações científicas realizadas por editoras prestigiadas como Nature, Plos, Wiley e Elsevier. Adicionalmente, realiza atividades em comunicação científica, e seu estúdio produz material literário, audiovisual e jogos com distribuição em mais de 40 países. Na área de Tecnologia e Inovação, possui diversos registros de Propriedade Intelectual no Instituto Nacional da Propriedade Industrial (INPI) e no *United States Patent and Trademark Office* (USPTO) e realiza parcerias com diversas instituições e empresas nacionais e internacionais nos setores público e privado.

Este manuscrito é dedicado à minha esposa, Aline M. Ghilardi,
sem a qual a minha existência até hoje não seria mais possível.

AGRADECIMENTOS

O presente trabalho foi realizado com apoio da Fundação de Amparo à Pesquisa do Estado de São Paulo (FAPESP), processo nº 2019/16727-3 ‘Paisagens Tafonômicas’. O presente trabalho foi realizado, também, com apoio do Conselho Nacional de Desenvolvimento Científico e Tecnológico (CNPq), processo nº 307333/2021-3; da iniciativa de divulgação científica “Colecionadores de Ossos”, e seus investidores; parte dos royalties da franquia “Dino Hazard” foram voltados para financiamento desta pesquisa; por fim, houve, também, investimento privado de Igor Lemos.

RESUMO

Dinossauros e demais avemetatarsálios compreendem um dos grupos de tetrápodes de maior sucesso. Eles são um ótimo modelo para estudar extremos evolutivos e como a vida reagiu a mudanças ambientais extremas os últimos 233 milhões de anos. Uma destas adaptações nos dinossauros saurísquios e nos pterossauros foi a Pneumatização do Esqueleto Pós-craniano (PSP), relacionada a um desenvolvido Sistema Respiratório semelhante aos sacos aéreos presentes nas aves. Divertículas projetam-se dos pulmões, resultando em um sofisticado sistema de refrigeração, com bastante disponibilidade de oxigênio no sangue. Isto resultou em uma vantagem evolutiva do grupo, permitindo-lhes suportar elevadas temperaturas imperantes no interior dos supercontinentes e, também, a manter o metabolismo acelerado. Contudo, por décadas permaneceu um enigma se a PSP teria surgido no ancestral comum dos avemetatarsálios, ou se pode ter surgido independentemente em diferentes grupos de dinossauros e pterossauros. Nos dinossauros, evidência de PSP não-ambígua está restrita aos Saurischia. Contudo, ainda não está elucidado até quão amplo filogeneticamente e o quão na base deste grupo ocorre a presença de PSP. Isto, porque, em organismos basais e distantes em relação aos Saurischia cretáceos, o registro da PSP não-ambígua é questionável nos fósseis, com base em observações macroscópicas. Este projeto almeja contribuir com esta temática em duas frentes de atuação. Primeiramente, busca avaliar as origens do sistema de sacos aéreos através do estudo de tecidos fossilizados (paleohistologia). Segundo, também aspira desenvolver um método mais robusto para identificação de traços destas divertículas em lâminas delgadas. Procurou-se por evidência de uma arquitetura trabecular óssea compatível com a presença não ambígua de sacos aéreos invasores do esqueleto. Para tal, utilizou-se microtomografia computadorizada para avaliar traços de divertículas pulmonares em fósseis de dinossauros iniciais do Triássico Superior da Bacia do Paraná. Paralelamente, foram avaliadas lâminas histológicas de diversos dinossauros, e um pterossauro, provenientes de diversas unidades do Cretáceo brasileiro. Os resultados deste projeto contribuem substancialmente para a resolução de um antigo enigma sobre a evolução, ao encontrar evidências para a ausência de sacos aéreos invasivos nos dinossauros mais antigos, do Carniano. Nesta tese também se apresenta a evidência mais cronologicamente antiga, e filogeneticamente inicial, de PSP não-ambígua, em um sauropodomorfo do início do Noriano. Portanto, nossos dados sugerem o fim da hipótese da homologia dos sacos aéreos invasivos e propõe múltiplas origens para a PSP em Avemetatarsalia, bem como apresenta a evolução gradual da pneumatização inicial em Sauropodomorpha. As lâminas delgadas, por outro lado, forneceram dados robustos para se estabelecer um método sólido para se diferenciar diferentes traços de tecidos moles no tecido ósseo, facilitando, objetivamente, a replicação destas análises em outros materiais ao redor do mundo.

Palavras-chave: Histologia; Petrologia; Mineralogia; Anatomia; Paleontologia

ABSTRACT

Dinosaurs and other avemetatarsalians comprise one of the most successful groups of tetrapods. They are a great model for studying evolutionary extremes and how life reacted to the changing environments over the last 233 million years. One of these adaptations in saurischian dinosaurs and pterosaurs was the Pneumatization of the Postcranial Skeleton (PSP), related to an evolved Respiratory System similar to the air sacs present in birds. Diverticula protrude from the lungs, resulting in a sophisticated refrigeration system, with plenty of oxygen available in the blood. This resulted in an evolutionary advantage for the group, allowing them to withstand the high temperatures prevailing within the supercontinents and maintain an accelerated metabolism. However, it is still an enigma whether PSP arose in the common ancestor of the avemetatarsalians, or if it may have emerged independently in different groups of dinosaurs and pterosaurs. In dinosaurs, evidence of non-ambiguous PSP is restricted to the Saurischia. However, it is not yet elucidated how phylogenetically broad and at the base of this group the presence of PSP occurs. This is because in organisms that are basal and distant from the Cretaceous Saurischia, the record of non-ambiguous PSP is questionable in fossils based on macroscopic observations. This project aims to contribute to this theme on two fronts. First, it seeks to evaluate the origins of the air sac system through the study of fossilized tissues (paleohistology). Second, it also aspires to develop a more robust method for identifying traces of these diverticula on thin sections. I searched for evidence of a trabecular bone architecture compatible with the non-ambiguous presence of invasive skeletal air sacs. To this end, computed microtomography was used to evaluate traces of pulmonary diverticula in early dinosaurs from the Upper Triassic of the Paraná Basin. Parallelly, I evaluated histological thin sections from several dinosaurs, and one pterosaur, from many units of the Brazilian Cretaceous. The results of this project contribute substantially to the resolution of an old enigma about evolution, by finding evidence for the absence of invasive air sacs in the oldest dinosaurs, from the Carnian. This thesis also presents the chronologically oldest, and phylogenetically earliest, evidence for a non-ambiguous PSP in an early Norian sauropodomorph. Therefore, our data suggests the end of the homology hypothesis for invasive air sacs, proposes multiple origins for PSP in Avemetatarsalia, and presents the gradual evolution of early pneumatization in Sauropodomorpha. The thin sections, on the other hand, provided robust data to establish a better method to differentiate different soft tissue traces in bone tissue, objectively facilitating the replication of these analyses in other materials around the world.

Keywords: Histology; Petrology; Mineralogy; Anatomy; Paleontology

SUMÁRIO

1 Introdução

1.1 Introdução à Paleohistologia

Paleohistologia é o estudo dos tecidos fossilizados para obtenção de informações da biologia e paleoecologia dos organismos, bem como informações paleoambientais e tafodiagenéticas (BUFFRÉNIL et al., 2021; CHINSAMY-TURAN, 2005; FRANCILLON-VIEILLOT et al., 1990; PADIAN; LAMM, 2013). É, portanto, uma metodologia de interface entre Biologia, Geologia, Medicina, Física e Química, e conceitos de todas estas áreas são necessários em diferentes graus, a depender da abordagem a se seguir.

É um campo intrigante da Paleontologia, que permite obter muitas informações até mesmo a partir de espécimes fragmentados, quase sempre subestimados quando primariamente estudados com objetivos restritos de taxonomistas e sistematas. Não obstante tem atraído novas pessoas para esta área ainda cheia de muitas lacunas para preencher.

Contudo, cautela é necessária no planejamento e condução das análises, pois boa parte dos estudos requerem uma abordagem destrutiva dos espécimes, ao seccionar fragmentos para preparo de lâminas delgadas. É recomendado que se realize muitas fotografias, réplicas e até mesmo digitalização 3D por tomografia computadorizada, antes de realizar as amostragens. CT scan é aconselhado como método de digitalização, ao invés de fotogrametria, pois a tomografia captura a natureza interna dos tecidos, o que é de suma importância para muitas possiblidades de abordagens que poderiam ser realizadas *a posteriori* (AURELIANO et al., 2018, 2020, 2021a).

Existe uma vasta gama de métodos e possibilidades para abordar. Mas é de suma importância que se tenha um objetivo claro, uma pergunta que compense ser respondida, sobretudo no caso de métodos destrutivos (LAMM, 2013b). É preferível a escolha de espécimes com a melhor identificação taxonômica possível. Entretanto, organismos indeterminados, mas com algum grau de identificação, também podem gerar *insights* interessantes com impacto em toda a evolução do grupo (CANALE et al., 2016; MARCHETTI et al., 2022; PADIAN; DE RICQLES; HORNER, 1995).

A composição química do tecido ósseo dos vertebrados é sempre uma cadeia constante de hidroxiapatita, que sobrevive à fossilização apenas incorporando alguns traços de elementos em sua estrutura (KAKEI et al., 2001; TRUEMAN; TUROSS, 2002). Contudo, o material orgânico de tecido mole é, na vasta maioria das situações, perdido, permitindo ingresso mecânico de grãos minerais e, também, de permineralização, ambos nas vacâncias antes preenchidas por sangue, tecidos gordurosos, dentre outros (AURELIANO et al., 2020; BAILLEUL et al., 2020).

Os dois tipos principais de tecido ósseo são o *compacta* e o *spongiosa*. O osso compacto é o mais denso e menos vascularizado, representado pelo córtex que reveste e protege o esqueleto. O osso esponjoso é composto por trabéculas delicadas, geralmente em contato com o sangue dentro das cavidades medulares os elementos apendiculares (HUTTENLOCKER; WOODWARD; HALL, 2013) e preenchendo o interior de vértebras e do crânio (CERDA; SALGADO; POWELL, 2012).

A paleohistologia possui uma escala de trabalho principal variando de milimétrica a micrométrica. Escalas menores já entram no campo de interesse maior da Cristalografia e Geoquímica (DUMONT et al., 2011; MÜRER et al., 2018).

Uma das principais abordagens, em vertebrados, é a esqueletocronologia. Trata-se da interpretação do estágio ontogenético no momento da morte do organismo. O padrão de vascularização dos tetrápodes muda desde o estágio embrionário até a senilidade. Existem várias revisões destas assinaturas, muitas vezes com enfoque em clados (FRANCILLON-VIELLOT et al., 1990; HUTTENLOCKER; WOODWARD; HALL, 2013; MITCHELL; SANDER, 2014; SANDER et al., 2011a).

Em uma escala de observação menor, a relação entre osso compacto (córtex) e osso esponjoso (medula preenchida por trabéculas) permite aferir como o tecido ósseo responde às pressões biomecânicas e ecológicas (FABBRI et al., 2022; HOUSSAYE, 2009; HOUSSAYE;

SANDER; KLEIN, 2016). Esta também é uma escala de observação interessante para o estudo de paleopatologias (HANNA, 2002; WOODRUFF et al., 2022).

1.2 Conceitos de Mineralogia Ótica aplicáveis à paleohistologia

O tecido ósseo, por se tratar de uma estrutura cristalizada, um biomineral, apresentará propriedades mineralógicas quando observado com o equipamento adequado. Na paleohistologia, as amostras são preparadas não como na histologia de organismos atuais, mas, sim, como na petrografia das Geociências (LAMM, 2013a).

A hidroxiapatita que compõe o osso é anisotrópica, isto é, apresenta diferentes propriedades em direções distintas de observação (KLEIN; DUTROW, 2007). Portanto, é necessário observar a lâmina paleohistológica ao microscópio petrográfico de luz polarizada para poder estudar a variação destes padrões nos tecidos cristalizados.

As principais ferramentas utilizadas para investigações são: a troca de lentes de aumento, onde, geralmente, não se ultrapassa o aumento de 20 X; o giro da platina, para observar a reação dos tecidos em diferentes ângulos de luz polarizada; cruzar os nicois, quando se quiser cruzar os feixes de luz; deixar os nicois paralelos, quando se quiser canalizar todo o feixe de luz polarizada. Como o tecido ósseo se trata apenas de um único mineral, independentemente da história tafodiagenética do organismo, nem todas as propriedades da Mineralogia Ótica observadas na vastidão de minerais inorgânicos serão úteis para estes estudos. Dentre as facetas mais úteis, pode-se destacar as listadas abaixo.

- Birrefringência. É uma propriedade ótica de minerais anisotrópicos, correspondente ao índice de refração da luz polarizada incidente (KLEIN; DUTROW, 2007). Na prática, são as cores que se observa na lente do microscópio, quando os nicois estão cruzados.
- Relevo ótico. É a característica de um mineral se destacar em relação a um corpo que o rodeia, também baseado em seu índice de refração (KLEIN; DUTROW, 2007). Normalmente observado com nicois paralelos. Minerais de relevo alto, possuem bordas notáveis e bem destacadas. Já os de relevo baixo, possuem suas delimitações bem sutis.
- Extinção ótica. É a maneira como o mineral se comporta ao girar a platina até o ponto de menor incidência de luz. Esta diminuição na intensidade de luz é o ângulo de extinção, que ocorre devido às propriedades cristalográficas do mineral (KLEIN; DUTROW, 2007).

Adicionalmente, pode se utilizar um compensador, quando observando em nicois cruzados. Isto amplia o comprimento de onda dos feixes de luz polarizada, intensificando a birrefringência, sendo excelente para detecção da matriz ao redor de ósteons secundários, indicando maturidade do canal vascular (Sistema Haversiano). Também é útil para fácil detecção de Fibras de Sharpey, cicatrizes de tendões.

1.3 Identificação de Pneumaticidade Esqueletal Pós-craniana (PSP)

Conforme mencionado no primeiro tópico desta tese, diversos autores têm aprimorado o método de detecção da presença de um sistema de sacos aéreos em organismos pretéritos, através da identificação de PSP não-ambígua (BRITT, 1994; O'CONNOR, 2006; WEDEL, 2003b; WEDEL; CIFELLI; SANDERS, 2000). O atual consenso sugere as seguintes condições para detecção de PSP não-ambígua em arcossauromorfos:

- Presença de lâminas vertebrais e fossas bem definidas;
- Presença de estruturas pneumáticas internas;

- Forames conectando ambas estruturas.

Adicionalmente, estudos mais recentes notaram que tem se discutido que o formato do forame também deve ser um fator a se levar em consideração (AURELIANO et al., 2022; TAYLOR; WEDEL, 2021). Sobretudo a largura dos forames, além dos seus posicionamentos nas vértebras, pode vir a ser um proxy adicional para diferenciação entre os pneumáticos e os nutricionais.

2 Artigos publicados e/ou a publicar

ARTIGO CIENTÍFICO

Aureliano, T., Ghilardi, A.M., Müller, R.T., Kerber, L., Pretto, F.A., Fernandes, M.A., Ricardi-Branco, F., Wedel, M.J.. 2022. The absence of an invasive air sacs system in the earliest dinosaurs suggests multiple origins of vertebral pneumaticity. *Scientific Reports* 12.1: 1-11.

Status: Manuscrito publicado na *Scientific Reports* no dia 09/12/2022

scientific reports

The absence of an invasive air sac system in the earliest dinosaurs suggests multiple origins of vertebral pneumaticity

Tito Aureliano[1,2,5], Aline M. Ghilardi[2], Rodrigo T. Müller[3,4], Leonardo Kerber[3,4], Flávio A. Pretto[3,4], Marcelo A. Fernandes[5], Fresia Ricardi-Branco[1] & Mathew J. Wedel[6]

The origin of the air sac system present in birds has been an enigma for decades. Skeletal pneumaticity related to an air sac system is present in both derived non-avian dinosaurs and pterosaurs. But the question remained open whether this was a shared trait present in the common avemetatarsalian ancestor. We analyzed three taxa from the Late Triassic of South Brazil, which are some of the oldest representatives of this clade (233.23 ± 0.73 Ma), including two sauropodomorphs and one herrerasaurid. All three taxa present shallow lateral fossae in the centra of their presacral vertebrae. Foramina are present in many of the fossae but at diminutive sizes consistent with neurovascular rather than pneumatic origin. Micro-tomography reveals a chaotic architecture of dense apneumatic bone tissue in all three taxa. The early sauropodomorphs showed more complex vascularity, which possibly served as the framework for the future camerate and camellate pneumatic structures of more derived saurischians. Finally, the evidence of the absence of postcranial skeletal pneumaticity in the oldest dinosaurs contradicts the homology hypothesis for an invasive diverticula system and suggests that this trait evolved independently at least 3 times in pterosaurs, theropods, and sauropodomorphs.

One of the key features that granted the successful evolution and diversification of birds is the postcranial skeletal pneumaticity (PSP) associated with an air sac system, allowing the derivation of lightweight hyperventilated bodies capable of flight[1–3]. Of particular importance are the pneumatic diverticula, air-filled epithelial protrusions of the lungs and respiratory air sacs. These diverticula permeate the body, leaving several traces of their interaction with the skeleton[4–6]. Such traces have been described in fossil taxa in three distinct avemetatarsalian clades: pterosaurs[7,8], sauropods[9–11] and theropods[12–14]. A crucial question is whether this trait is homologous to ornithodirans, or developed independently two or three times in this group[15–17]. O'Connor[3] proposed a method to evaluate unambiguous evidence of PSP in the fossil record. These three rules consist in observing three lines of evidence: the presence of well-developed fossae and laminae; the evidence of foramina inside these fossae; and the connection of these foramina with internal pneumatic structures (e.g. chambers, camerae, camellae). Novel computed tomography technologies and new key fossils from South America now allow us to address this long-standing enigma. A recently-described dinosaur fauna from the Late Triassic (early Carnian Candelária Sequence, Santa Maria Formation) of South Brazil accounts for the oldest dated taxa of this clade (233.23 ± 0.73[18]). In this study, we analyzed the axial skeletons of the early diverging sauropodomorphs *Buriolestes*[19] and *Pampadromaeus*[20], and the herrerasaurid *Gnathovorax*[21] to evaluate the presence of unambiguous PSP and discuss the evolution of PSP in avemetatarsalians.

[1]Institute of Geosciences, University of Campinas (Unicamp), Campinas, Brazil. [2]Diversity, Ichnology and Osteohistology Laboratory (DINOlab), Department of Geology, Federal University of Rio Grande Do Norte (URFN), Natal, Brazil. [3]Centro de Apoio À Pesquisa Paleontológica da Quarta Colônia (CAPPA), Federal University of Santa Maria (CAPPA/UFSM), São João Do Polêsine, Brazil. [4]Programa de Pós-Graduação Em Biodiversidade Animal,

Federal University of Santa Maria (UFSM), Santa Maria, Brazil. [5]Laboratório de Paleoecologia E Paleoicnologia (LPP), Departamento de Ecologia E Biologia Evolutiva (DEBE), Federal University of São Carlos (UFSCar), São Carlos, Brazil. [6]College of Osteopathic Medicine of the Pacific and College of Podiatric Medicine, Western University of Health Sciences, Pomona, USA. 👍✇email: aureliano.tito@gmail.com

Materials and method

Institutional abbreviations. CAPPA/UFSM, Centro de Apoio à Pesquisa Paleontológica da Quarta Colônia, Universidade Federal de Santa Maria, São João do Polêsine, Rio Grande do Sul, Brazil; LPP-PV, Laboratório de Paleoecologia e Paleoicnologia (UFSCar), Federal University of São Carlos (UFSCar), São Carlos, São Paulo, Brazil; OMNH, Oklahoma Museum of Natural History, Norman, Oklahoma, United States of America; PVL, Paleovertebrate collection, Instituto "Miguel Lillo", San Miguel de Tucumán, Salta, Argentina; MPCA, Museo Municipal de Ciencias Naturales "Carlos Ameghino", Mercedes, Buenos Aires, Argentina; MOR, Museum of the Rockies, Bozeman, Montana, United States of America; NHM, Natural History Museum, London, United Kingdom; ULBRA, Centro de Apoio à Pesquisa Paleontológica da Quarta Colônia, Universidade Federal de Santa Maria, São João do Polêsine, Rio Grande do Sul, Brazil (previously Museu de Ciências Naturais, Universidade Luterana do Brasil, Canoas, Brazil).

Specimens. The studied specimen of *Buriolestes schultzi* (CAPPA/UFSM 0035) corresponds to a nearly complete articulated skeleton and one of the best-known early dinosaurs[19]. It is one of the oldest sauropodomorphs and the basalmost taxon within this clade (but see[22]). The holotype of *Gnathovorax cabreirai* (CAPPA/UFSM-0009) corresponds to a nearly complete articulated skeleton, with some dorsal axial segments still under preparation[21]. It is one of the oldest and best-preserved herrerasaurids ever found to date. The holotype of *Pampadromaeus barberenai* (ULBRA-PV016) is an unarticulated almost complete skeleton[20]. Since the ULBRA collection was closed, ULBRA-PV016 is now housed in CAPPA/UFSM. Whereas histological thin sections were not performed, some structures demonstrate that all specimens reached an advanced degree of skeletal maturity, indicating that they were not juveniles at the time of death. Such evidence is based on the neurocentral sutures, the presence and shape of some muscle attachment structures, such as the femoral trochanteric shelf and anterolateral scar in the proximal portion of the femur, and dorsolateral trochanter[23–25].

Locality and horizon. *Buriolestes* was excavated at the Buriol Site (29°39′34.2″ S, 53°25′47.4″ W) and *Gnathovorax* at the Marchezan Site (29°37′52″ S, 53°27′02″ W), both at São João do Polêsine municipality, Rio Grande do Sul state, South Brazil. These sites are part of the Alemoa Member, Upper Triassic (Carnian) Santa Maria Formation, Paraná Basin. Their silty sandstone beds are included in the *Hyperodapedon* Assemblage Zone within the Acme Zone[26], and absolute zircon dating for these beds points to 233.23 ± 0.73 Ma[18]. *Pampadromaeus* was collected at the "Várzea do Agudo" (=Janner) Site (29°39′10.89″ S, 53°17′34.20″ W), Agudo municipality, also Rio Grande do Sul state. The context is also the Alemoa Member, *Hyperodapedon* Assemblage, but at the immediately overlaying *Exaeretodon* Sub-zone stratum[20]. Therefore, it is known that *Pampadromaeus* pertained to a faunal assemblage slightly more recent than that of *Buriolestes* and *Gnathovorax* (see Fig. 1).

Taphonomic remarks. CAPPA/UFSM 0035 and 0009 were not significantly affected by taphonomic compression, whereas several bone elements of ULBRA-PV016 are diagenetically distorted, not reflecting their natural shape. Nevertheless, the external texture of the elements of ULBRA-PV016, as well as that of the other two specimens, is well-preserved, depicting fine details of its anatomy. Opaque diagenetic minerals are also present in CAPPA/UFSM 0035 and 0009 as well as moderate calcite permineralization.

Anatomical nomenclature. Wilson's nomenclature was applied for vertebral laminae and fossae[6,27,28] and Wedel's terminology for vertebral pneumatic structures[5,29,30]. We followed O'Connor's method to identify unambiguous evidence of PSP in our specimens[3]. Figure 1 exemplifies vertebrae of extinct and living taxa, and indicates structures such as laminae and fossae, illustrating different types of pneumatic and apneumatic architectures.

Micro-computed tomography (µCT scan). The anterior (third) cervical vertebra and an articulated posterior cervical vertebra of *Gnathovorax* were scanned. Dorsals are still under preparation in the jacket and were not available for this analysis. Almost the entire cervical series of *Buriolestes* was scanned as well as two middle dorsals. Finally, the three available dorsal vertebrae of *Pampadromaeus* were scanned.

Specimens were scanned on a Bruker-Skyscan 1173 microtomographer equipped with a 130-kV µ-focus X-ray source with a voxel size of 0.15 mm. The procedure took place at the *Instituto do Petróleo e dos Recursos Naturais* at the Universidade Católica do Rio Grande do Sul/PUCRS), Porto Alegre (Brazil). *3D-Slicer* v5.2[31] and *CloudCompare* v2.9.1[32] were used to analyze the data by applying color grades based on bone tissue density[33]. Digital measurements were taken with *ImageJ* v1.52[34]. All microtomography data was uploaded to the Morphobank platform and is available through this link: http://morphobank.org/permalink/?P4477.

Results

The neural arches of the three taxa show laminae and fossae with moderate complexity compared to what is observed in derived saurischians. *Gnathovorax* presents more robust vertebrae with deeper lateral fossae at the centra than the sauropodomorphs. *Buriolestes* and *Pampadromaeus* vertebrae are rather laterally shorter in anterior view with very subtle lateral fossae in the centra (if any). Pneumatic foramina are absent. However, tiny nutritional foramina abound in almost every element and vary little throughout the vertebral series (Figs. 2, 3). These foramina appear singly, in pairs, and in trios, with no discernible patterns. Lateral foramina present a much greater variance in diameter (0.01–0.9 mm) than the ones occurring ventrally (0.3–0.5 mm). This contrast in size reaches an extreme in the cervicals of *Gnathovorax*, where the ventral foramina (Fig. 3C) are up to ten

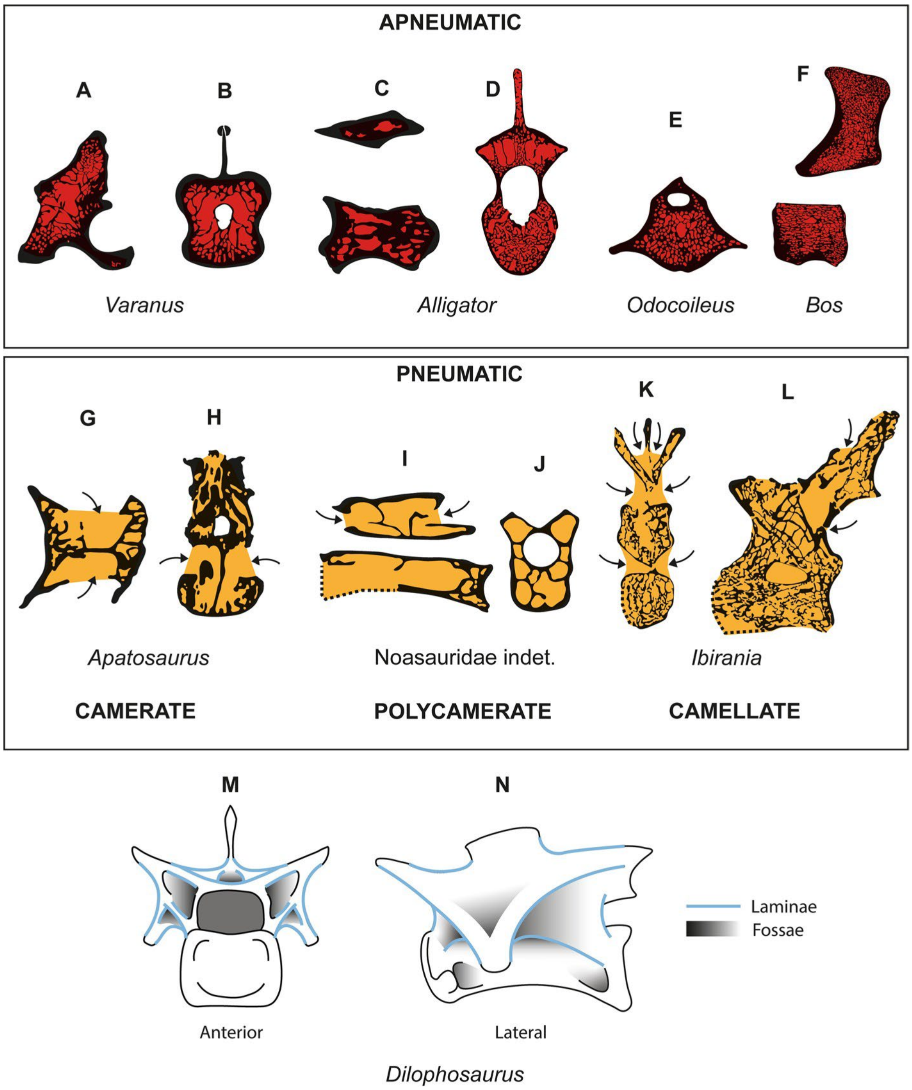

Figure 1. Examples of vertebrae with apneumatic (**A**–**F**) and pneumatic (**G**–**L**) architectures, and schematic drawings of vertebral fossae and laminae in (**M** and **N**). (**A**,**B**) *Varanus komodoensis* (NHMUK RR 1934.9.2.2)[15]. (**C**,**D**) *Alligator mississippiensis* (OUVC 11415 and NHMUK RR 1975.14.23, respectively). (**E**) *Odocoeileus virginianus*. (**F**) *Bos taurus*. (**G**,**H**) *Apatosaurus* sp. (MOR 957 6-29-92)[35]. (**I**,**J**) noasauridae indet. (DGM 929-R)[36]. (**K**,**L**) *Ibirania parva* (LPP-PV-0200)[37]. (**M**,**N**) *Dilophosaurus wetherilli*[38]. Lateral view in (**A**,**C**,**F**,**I**,**L**,**N**). Transverse sections in (**B**,**D**,**E**,**J**,**K**,**M**). Ventral view in (**G**). High contrast outlines in A-D and G-L based on CT scan data. (**M** and **N**) are based on the original schematic drawing of Adam Marsh[38]. WitmerLab at Ohio University provided access to the *Alligator* data originally appearing on their website, the collection of which was funded by NSF. The file was downloaded from www.MorphoSource.org, Duke University. Not to scale. Figures were generated with Adobe Illustrator CC version 22 X64.

times broader than the ones occurring inside the lateral fossa (Fig. 3E,F). See the Supplementary Materials for measurements.

Taphonomy greatly affected some vertebrae and, consequently, influenced some μCT scan slices. Sometimes such differences occur within the same specimen (as in *Buriolestes* and *Pampadromaeus*; Figs. 4, 6). Nonetheless, the data obtained from this analysis successfully provide information on the internal architecture of the vertebrae in all three taxa (Figs. 4, 5, 6). The neural arches feature a homogenous texture of dense trabeculae in all specimens, and the greatest structural diversity is located inside the centra. These comprise mostly apneumatic chaotic trabeculae (ctr; Figs. 4, 5, 6). There are non-pneumatic chambers (ccv) inside certain elements of *Buriolestes* (Fig. 4E,H–M) and *Gnathovorax* (Fig. 5D,F,H,J–M). Small circumferential chambers (cc) populate the centra dorsally in all specimens (Fig. 4J; Fig. 5D,J,M; Fig. 6H) and also laterally in the pedicles in *Buriolestes*

(Fig. 4D). Two layered trabeculae (ltr) are present in the cotyles of both sauropodomorphs but not in the herrerasaurid. *Pampadromaeus* features a 'pseudo-polycamerate' (ppc) architecture (Fig. 6L). Here we define 'pseudo-polycamerate' as chaotic apneumatic trabecular chambers infilled with blood and fat tissues but resemble the fractals of the pneumatic polycamerate as defined by Wedel[29]. Figure 7 illustrates both architectures side-by-side

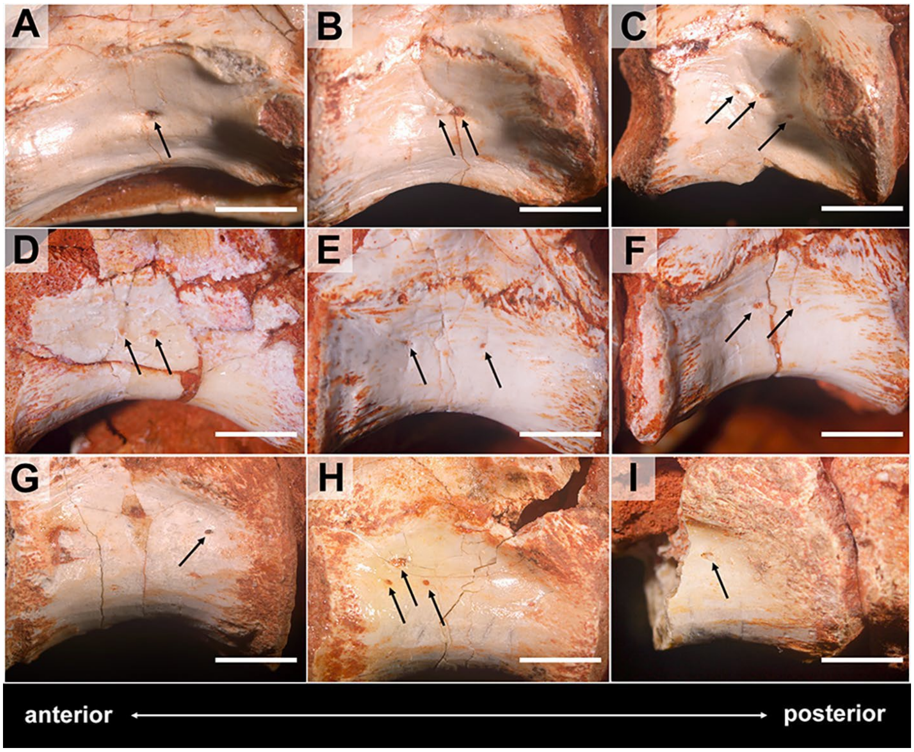

Figure 2. Detail of the vertebrae and foramina of the basalmost sauropodomorph *Buriolestes* (CAPPA/UFSM-0035). Cervical (**A–C**), anterior (**D–F**) and posterior (**G–I**) dorsal vertebrae in right lateral view. Note that nutritional foramina are present throughout the axial skeleton (dark arrows). Anterior/posterior orientation was defined based on the axial position, not the anatomical plane. Scale bar = 5 mm. Figures were generated with Adobe Photoshop CC version 22.5.1 X64.

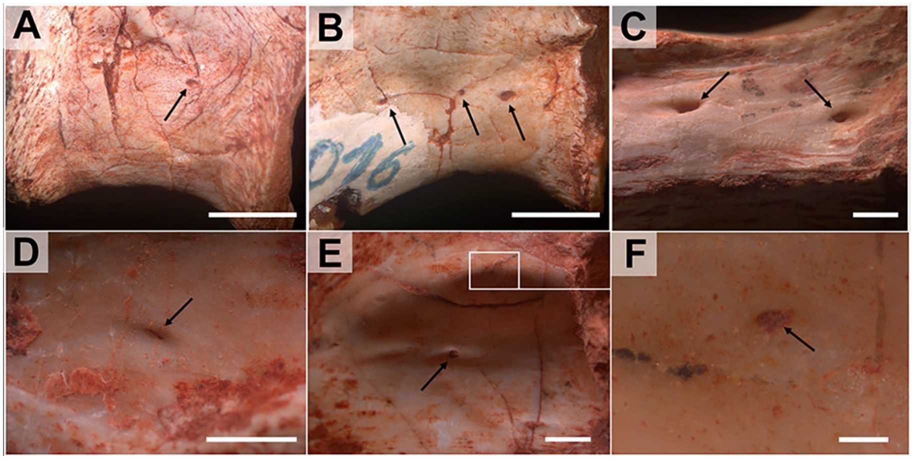

Figure 3. Detail of the vertebrae and foramina of the early sauropodomorph *Pampadromaeus* (ULBRA-PV016; (**A**,**B**)) and the herrerasaurid *Gnathovorax* (CAPPA/UFSM-0009; (**C–F**)). Anterior dorsal vertebrae in (**A**,**B**). Anterior cervical in **C** and posterior cervical in (**D–F**). Nutritional foramina are present on the lateral surface

of the centra (small arrows) in (**A**,**B**) and (**D**–**F**. They present a diminutive diameter when located inside the lateral fossae (**D**–**F**) and are broader on the ventral portion of the centra (**C**). Scale bar in (**A**,**B**)=5 mm; in (**C**–**E**)=1 mm; in (**F**)=0.1 mm. Figures were generated with Adobe Photoshop CC version 22.5.1 X64.

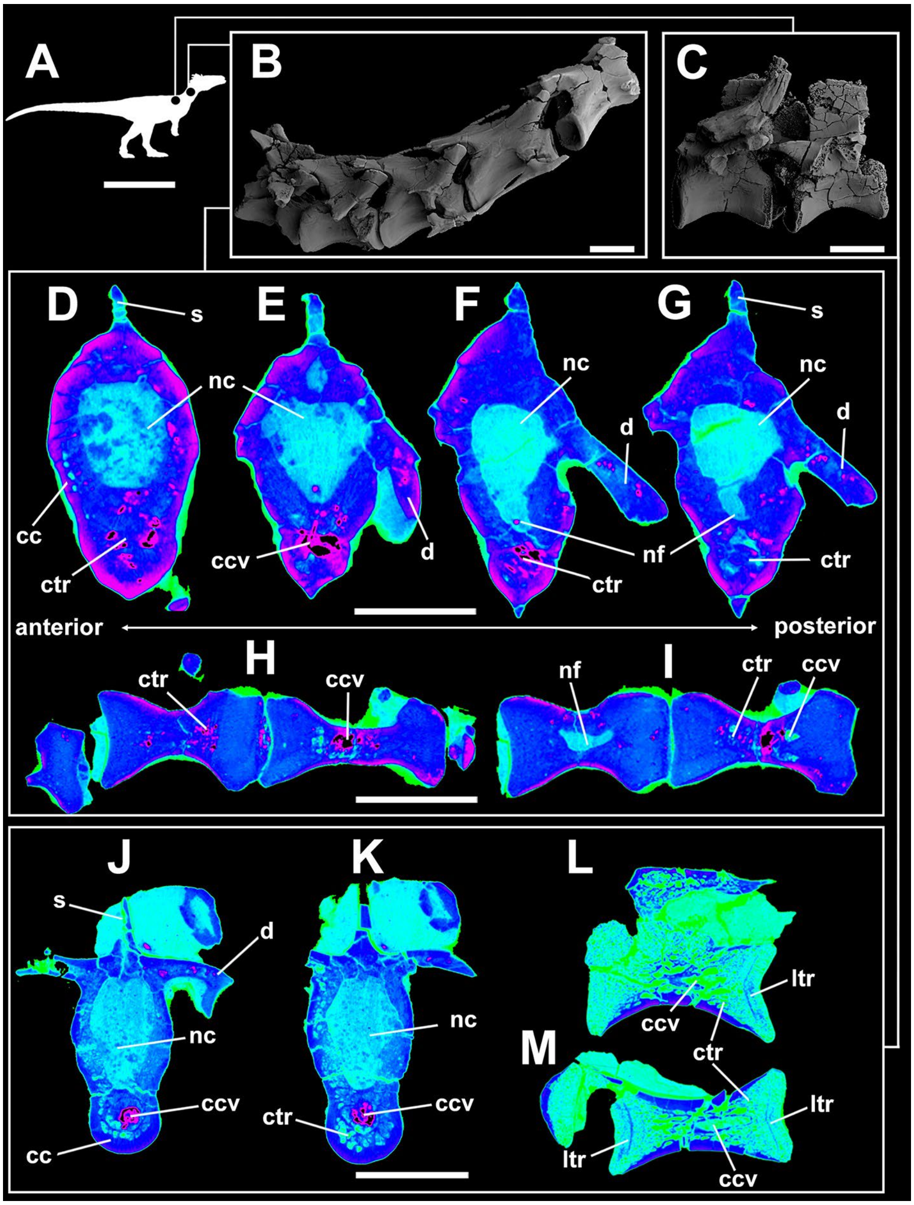

Figure 4. Micro-computed tomography of the vertebrae of the basalmost sauropodomorph *Buriolestes* (CAPPA/UFSM 0035). (**A**) silhouette shows the position of the axial elements. Artist: Felipe Elias. (**B**), three-dimensional reconstruction of the articulated cervical vertebral series and the correspondent high-contrast density slices in (**D–I**). Diagenetic processes partially compromised the internal structures in these cervicals. (**C**), 3D reconstruction of the articulated anterior dorsal vertebrae and the correspondent high-contrast density slices in (**J–M**). Small circumferential chambers occur both ventrally in the dorsal centrum (**J**) and laterally in the neural arch pedicles (**D**). All images indicate apneumatic chaotic trabeculae architecture. Some of the latter develop into larger chambers in the centrum (**E**,**J**,**K**). Nutritional foramina are broader at the bottom of the neural canal in the posterior cervicals (**F**,**G**). All slices were taken from the approximate midshaft. Anterior views in (**D–H**,**J**,**K**). Lateral view in (**L**). Ventral view in (**H**,**I**,**M**). Anterior/posterior orientation was defined based on the axial position, not the anatomical plane. *cc* circumferential chamber, *ccv* chamber in the centrum, *ctr* chaotic trabecula, *d* diapophysis, *ltr* layered trabeculae, *nc* neural canal, *nf* nutritional foramen, *s* neural spine. Scale bar in (**A**)=500 mm; in (**B–M**)=10 mm. Computed tomography data processed with 3D Slicer version 4.10. Figures were generated with Adobe Photoshop CC version 22.5.1 X64.

in high-contrast monochromatic vertebral profiles. Something similar exists in the earlier *Buriolestes* but the configuration, in this case, is rather a combination of chaotic trabeculae and elongated chambers (Fig. 3L,M). Finally, the neural canal nutritional foramina are broader towards the dorsal-cervical joint, as shown in *Buriolestes*

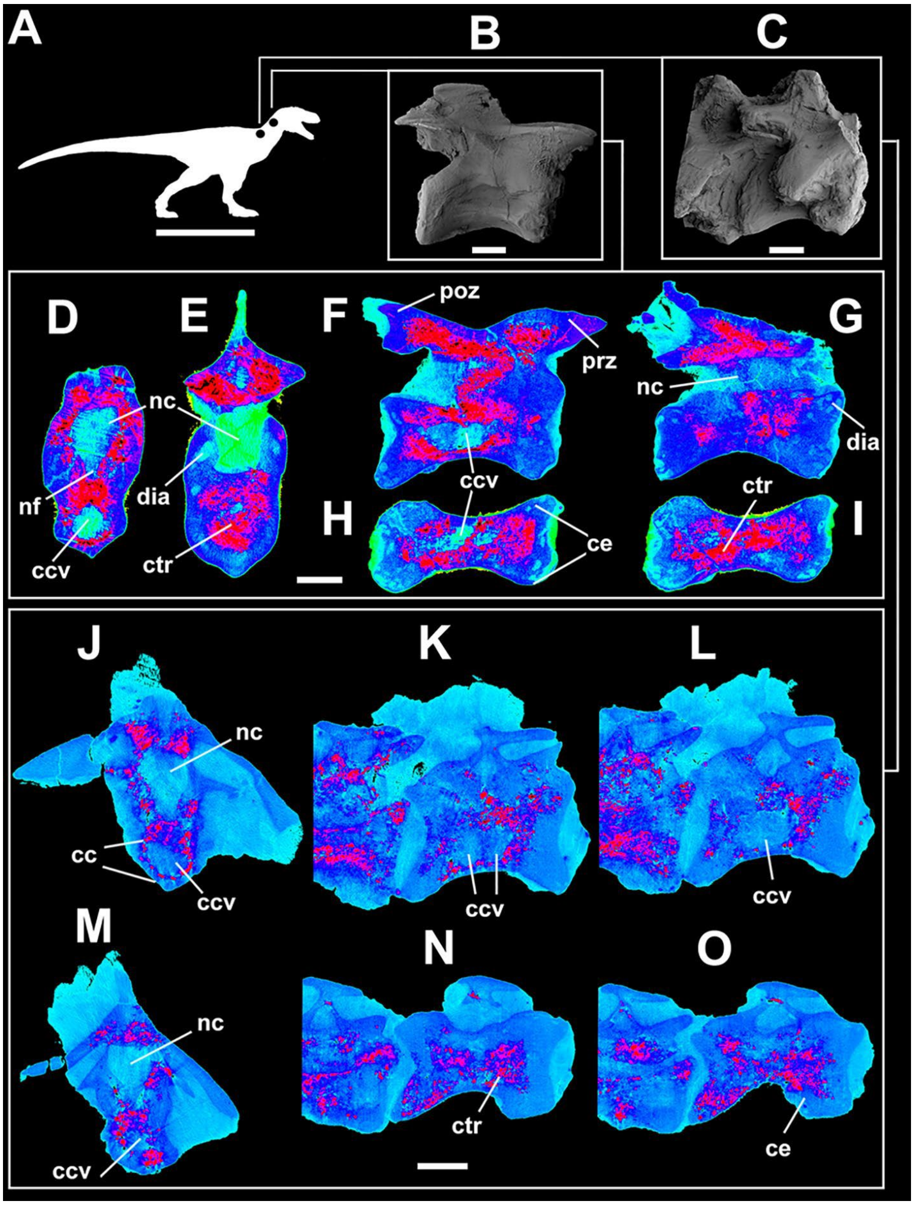

Figure 5. Micro-computed tomography of the vertebrae of the herrerasaurid *Gnathovorax* (CAPPA/UFSM-0009). (**A**) silhouette shows the position of the axial elements. Artist: Felipe Elias. (**B**) 3D reconstruction of the anterior cervical vertebra and the correspondent high-contrast density slices in (**D-I**). Diagenetic artifacts greatly compromised the internal structures. (**C**) 3D reconstruction of the articulated posterior cervical vertebrae and the correspondent high-contrast density slices in (**J–O**). Minerals infilled between trabecular vacancies generate reddish anomalies. All images indicate irregular, chaotic, apneumatic architecture. Note the apneumatic large chambers in the centrum (ccv) and the smaller circumferential chambers at the bottom (cc). All slices were taken from the approximate midshaft. Anterior views in (**D**,**H**,**I**). Right lateral view in (**E**,**L**,**M**). Ventral view in (**F**,**G**,**J**,**K**). *cc* circumferential chambers, *ccv* chamber in the centrum, *ce* centrum, *ctr* chaotic trabeculae, *d* diapophysis, *dia* diagenetic artifact, *nc* neural canal, *nf* nutritional foramen, *poz* postzygapophysis, *prz* prezygapophysis. Scale bar in (**A**) = 1000 mm; in (**B**–**O**) = 10 mm. Computed tomography data processed with 3D Slicer version 4.10. Figures were generated with Adobe Photoshop CC version 22.5.1 X64.

and *Gnathovorax* (Fig. 4D–G and Fig. 5D,J,M). These large vascular foramina in the floor of the neural canal were probably associated with the basivertebral venous system[39,40].

Discussion

The microtomography of the three specimens evidences the absence of unambiguous PSP. Our data also support that a better description of the foramen anatomy can solve questions on ambiguous PSP[41]. Tiny foramina (<1 mm) inside weakly developed fossae are vascular in origin instead of indicative of pneumatization[3,41].

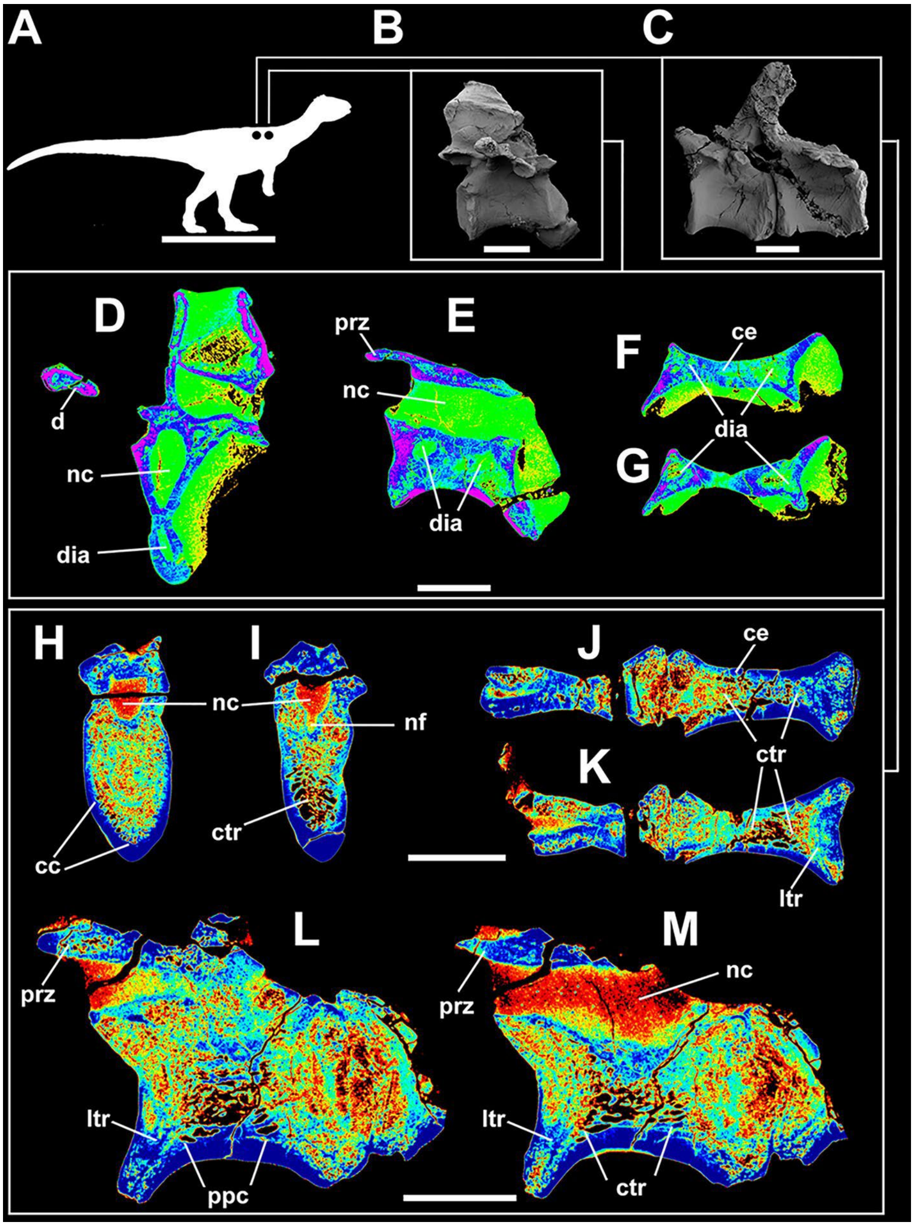

Figure 6. Micro-computed tomography of the vertebrae of the early sauropodomorph *Pampadromaeus* (ULBRA-PV016). (**A**) silhouette shows the position of the axial elements. Artist: Felipe Elias. (**B**) 3D reconstruction of the mid-dorsal vertebra and the correspondent high-contrast density slices in (**D**–**G**). Diagenetic artifacts significantly compromised the internal structures in this element. (**C**) 3D reconstruction of the articulated anterior dorsal vertebrae and the correspondent high-contrast density slices in (**H**–**M**). Note the circumferential chambers at the bottom of the centrum in (**H**). Also, note the 'pseudopolycamerate' architecture in (**L**). All images indicate irregular, chaotic, apneumatic architecture. All slices were taken from the approximate midshaft. Anterior views in (**D**,**H**,**I**). Right lateral view in (**E**,**L**,**M**). Ventral view in (**F**,**G**,**J**,**K**). *cc* circumferential chambers, *ce* centrum, *ctr* chaotic trabeculae, *d* diapophysis, *dia* diagenetic artifact, *ltr* layered trabeculae, *nc* neural canal, *nf* nutritional foramen, *ppc* 'pseudopolycamerate' architecture, *prz* prezygapophysis. Scale bar in (**A**) = 500 mm; in (**B**–**M**) = 10 mm. Computed tomography data processed with 3D Slicer version 4.10. Figures were generated with Adobe Photoshop CC version 22.5.1 X64.

Proportionally large-diameter foramina (e.g., > 5 mm, in our specimens) associated with deep fossae must be taken into consideration when diagnosing unambiguous PSP[3,41]. Those latter must also be connected with clear internal pneumatic architecture[3,30,41]. Most pneumatic vertebrae are internally organized into camerate and camellate bone tissues, and these are the best macroscopic correlates of bone-penetrating pneumatic diverticula[11,13,29,36,37,42,43]. These Carnian taxa failed to show an architecture consistent with pneumatization, such as that observed in the derived sauropods *Saltasaurus* (PVL 4017–17/214)[11] and *Ibirania* (LPP-PV-0200)[37], and theropods like *Aoniraptor* (MPCA-Pv 804/1-25)[43] and noasaurids (DGM 929-R)[36]. Even giant basal neosauropods

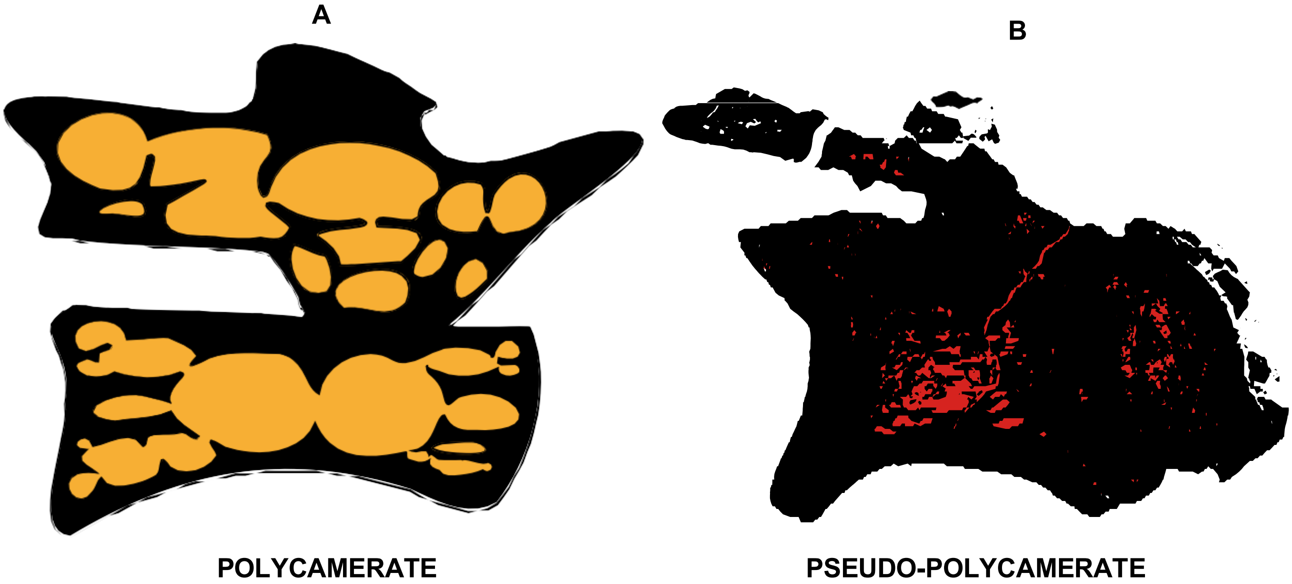

Figure 7. Schematic profile of the internal architecture of two saurischians. (**A**) *Dilophosaurus*, showing a polycamerate pneumatic structure. (**B**) *Pampadromaeus*, demonstrating pseudo-polycamerate apneumatic trabeculae. (**A**) is based on Marsh[38] and Brum et al.[36]. Not to scale. Figures were generated with Adobe Illustrator CC version 20 X64.

such as *Apatosaurus* (OMNH 01094)[10] and *Giraffatitan* (MB.R. 2180.25/26)[44] present large organized cortical-tissue camerae suggesting interaction with pneumatic diverticula. Lastly, our data indicate that an invasive pneumatic system was not present in the postcranial skeletons of the earliest Carnian dinosaurs. The earliest evidence of PSP occurred in the fossae adjacent to the diapophysis in most basal sauropodomorphs[45]. Our scans show that in *Buriolestes*, *Pampadromaeus*, and *Gnathovorax* any fossae associated with the neural arches or diapophyses are shallow, simple (i.e., not divided into subfossae sensu Wilson[27]), and do not represent invasive pneumatization of the vertebrae.

The evidence of the absence of PSP in the earliest dinosaurs suggests that invasive PSP found in theropods, sauropods and pterosaurs was not homologous[3,15,30,46,47]. This is solid evidence that invasive intraosseous pneumatization must have evolved at least three times independently (see Fig. 8). Our results are also in accordance with recent findings that demonstrate the nonexistence of PSP in the early ornithischian *Heterodontosaurus*[47]. Nonetheless, this still does not exclude the hypothesis indicating that the homology of the underlying non-invasive pulmonary tissue could be an ancestral ornithodiran condition[15,48]. In extant birds, many diverticula do not interact with the skeleton, including intermuscular, intervisceral, and subcutaneous diverticula[49]. However, similar 'cryptic' diverticula[50] in basal ornithodirans would be unlikely to preserve in the Triassic fossil record, and by definition, such diverticula do not leave diagnostic skeletal traces, and both of these factors complicate any attempts to investigate the earliest stages in the evolution of PSP. Even histological evidence of the respiratory diverticula requires interaction with the bone to survive fossilization[4,33,37,43,51].

Some early non-archosaurian archosauriforms such as *Erythrosuchus* present developed fossae, laminae, and even foramina which led some authors to propose ancestral evidence of PSP[52]. However, we suggest a careful analysis of foramina size and position, as well as a detailed description of the internal trabecular architecture. These are the definitive macroscopic indicators of unambiguous PSP, as previously hypothesized[3,30,41]. *Erythrosuchus* microCT scan (NHMUK R3592)[15] revealed a chaotic array of trabecular walls in a very dense, near-granular, mass of thick bone throughout the vertebra (Fig. 6 in[15]). Additionally, the absence of connections between internal structures with external foramina corroborates with the apneumatic status of *Erythrosuchus*[15].

The short time and phylogenetic distances between the early sauropodomorph *Buriolestes* and the later *Pampadromaeus* allowed the observation of a short step in the evolution of vertebral vasculature. The increasingly irrigated internal architecture with chaotic trabecular vacancies and chambers in basal dinosaurs, filled with blood and fat tissues, could have favored the evolution of the true pneumatic structures in the latest Triassic. *Pampadromaeus* was excavated in a stratum slightly younger than *Buriolestes* and presented a pseudo-polycamerate vascularized architecture, much different from the chaotically organized pattern of the older *Buriolestes*. This change demonstrates the increasing complexity of these tissues that may have laid the groundwork for the later origin of true unambiguous PSP.

We note many suggestive correspondences between the apneumatic vertebral internal structure of these Carnian dinosaurs and the pneumatic internal structures of more derived saurischians. Similar apneumatic chambers were also described in the vertebral centra of non-avemetarsalian archosauromorphs such as in the centra of the

Alligator (see Fig. 1C,D) and in the neural arches of taxa such as *Erythrosuchus*[15]. In early saurischians, in addition to the pseudo-polycamerate architecture discussed above, apneumatic chambers in the centra (ccv) of the Carnian taxa are structurally similar to pneumatic camerae of later sauropods and theropods (Fig. 6)[29]. Even more compellingly, small circumferential chambers (cc) and layered trabeculae (ltr) in these early dinosaurs resemble

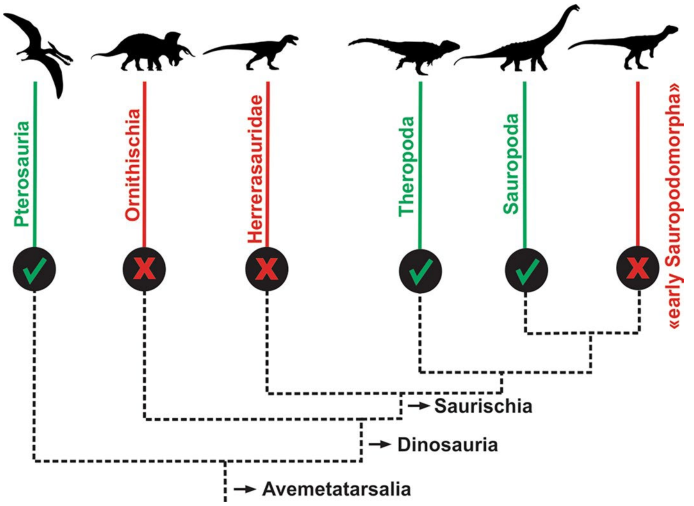

Figure 8. A simplified cladogram of Avemetatarsalia illustrates the branches in which the unambiguous presence of an air sacs system has been evidenced (bright/green 'check' sign). The absence of an air sacs system in the oldest dinosaurs presented in this study eliminates the hypothesis of the homology of this trait between pterosaurs and saurischians. Our results also corroborate that this trait appeared independently in three clades: Pterosauria, Theropoda, and Sauropoda. "Early Sauropodomorpha" is a paraphyletic branch. Cladogram based on Novas et al.[54]. Silhouettes authored by Felipe Elias, Scott Hartman, Tasman Dixon, Jagged Fang, and FunkMonk. Figures were generated with Corel Draw X6 version.

circumferential pneumatic chambers and radial camellae in derived titanosaurian sauropods[37]. In extant birds, developing pneumatic diverticula have been observed to follow pre-existing blood vessels[3,53]. If pneumatization followed vascular pathways in extinct dinosaurs[41], that could explain why pneumatic internal structures in later, more derived dinosaurs resemble the ancestral, apneumatic structures documented in this study. A detailed study of the ontogenetic development of vertebral pneumaticity in a derived sauropod or non-avian theropod, using CT and bone histology, is needed to elucidate the relationship between pneumatic internal structures and the apneumatic structures that predate them (ontogenetically and phylogenetically).

Eventually, the analysis of Norian bagualosaurian taxa will have the potential to provide evidence of the rise of unambiguous PSP, and the appearance of the invasive pneumatic system that we observe in later avemetatarsalians, including extant birds.

Conclusions

We analyzed three of the earliest dinosaurs and our data fill a gap in the knowledge of the evolution of the Respiratory System. Selected highlights are listed below:

- Microtomography of the three specimens indicates the absence of unambiguous postcranial pneumaticity. Therefore, we conclude that an air sacs system permeating the skeleton was not present in the earliest dinosaurs (late Carnian).
- The evidence of the absence of PSP in the earliest saurischian dinosaurs corroborates the hypothesis that the invasive air sac systems found in theropods, sauropods and pterosaurs were not homologous. This is solid evidence that unambiguous PSP evolved at least three times independently in those clades. Nonetheless, this still does not exclude the other hypothesis indicating that the homology of the underlying pulmonary tissue could be an ancestral ornithodiran condition.
- The chaotic organization of the larger internal trabecular vacancies and chambers, originally filled with blood and fat tissues, could have favored the evolution of the true pneumatic structures in the latest Triassic. *Pampadromaeus* was slightly younger than *Buriolestes* and already presented a pseudo-polycamerate structure, supporting the increasing complexity of these tissues that would later favor the origin of true unambiguous PSP.

Finally, investigations regarding Norian taxa are crucial in order to provide evidence on the rise of unambiguous PSP, and the appearance of the air sacs system as we know it today from the surviving avemetatarsalians (see Table S1 in supplementary materials).

Data availability

All fossils are housed in a public research institution and can be accessed with a request to the curator of the collection. Microtomography data are available upon request by email to the corresponding author.

Received: 3 October 2022; Accepted: 24 November 2022

References

1. Proctor, N. S. & Lynch, P. J. *Manual of Ornithology: Avian Structure & Function* (Yale University Press, 1993).
2. Britt, B. B., Makovicky, P. J., Gauthier, J. & Bonde, N. Postcranial pneumatization in Archaeopteryx. *Nature* **395**, 374–376 (1998).
3. O'Connor, P. M. Postcranial pneumaticity: An evaluation of soft-tissue influences on the postcranial skeleton and the reconstruction of pulmonary anatomy in archosaurs. *J. Morphol.* **267**, 1199–1226 (2006).
4. Lambertz, M., Bertozzo, F. & Sander, P. M. Bone histological correlates for air sacs and their implications for understanding the origin of the dinosaurian respiratory system. *Biol. Lett.* **14**, 20170514 (2018).
5. Wedel, M. J. Vertebral pneumaticity, air sacs and the physiology of sauropod dinosaurs. *Paleobiology* **29**, 243–255 (2003).
6. Wilson, J. A. *New Vertebral Laminae and Patterns of Serial Variation in Vertebral Laminae of Sauropod Dinosaurs* (Museum of Paleontology, The University of Michigan, 91–110 (2012).
7. Buchmann, R. & Rodrigues, T. The evolution of pneumatic foramina in pterosaur vertebrae. *An. Acad. Bras. Cienc.* **91**(Suppl 2), e20180782 (2019).
8. Butler, R. J., Barrett, P. M. & Gower, D. J. Postcranial skeletal pneumaticity and air-sacs in the earliest pterosaurs. *Biol. Lett.* **5**, 557–560 (2009).
9. Wedel, M. J. The evolution of vertebral pneumaticity in sauropod dinosaurs. *J. Vert. Paleontol.* **23**, 344–357 (2003).
10. Woodward, H. N. & Lehman, T. M. Bone histology and microanatomy of *Alamosaurus sanjuanensis* (Sauropoda: Titanosauria) from the maastrichtian of Big Bend National Park Texas. *J. Vert. Paleontol.* **29**, 807–821 (2009).
11. Cerda, I. A., Salgado, L. & Powell, J. E. Extreme postcranial pneumaticity in sauropod dinosaurs from South America. *Paläontol. Z.* **86**, 441–449 (2012).
12. Gianechini, F. A. & Zurriaguz, V. L. Vertebral pneumaticity of the paravian theropod *Unenlagia comahuensis*, from the Upper Cretaceous of Patagonia, Argentina. *Cretaceous Res.* **127**, 104925 (2021).
13. O'Connor, P. M. The postcranial axial skeleton of *Majungasaurus cretanissimus* (Theropoda: Abelisauridae) from the Late Cretaceous of Madagascar. *J. Vert. Paleontol.* **27**, 127–163 (2007).
14. Schachner, E. R., Lyson, T. R. & Dodson, P. Evolution of the respiratory system in nonavian theropods: Evidence from rib and vertebral morphology. *Anat. Rec.* **292**, 1501–1513 (2009).
15. Butler, R. J., Barrett, P. M. & Gower, D. J. Reassessment of the evidence for postcranial skeletal pneumaticity in Triassic archosaurs, and the early evolution of the avian respiratory system. *PLoS ONE* **7**, e34094 (2012).
16. Brocklehurst, R. J., Schachner, E. R., Codd, J. R. & Sellers, W. I. Respiratory evolution in archosaurs. *Philos. Trans. R. Soc. Lond. B Biol. Sci.* **375**, 20190140 (2020).
17. Schachner, E. R., Farmer, C. G., McDonald, A. T. & Dodson, P. Evolution of the dinosauriform respiratory apparatus: New evidence from the postcranial axial skeleton. *Anat. Rec.* **294**, 1532–1547 (2011).
18. Langer, M. C., Ramezani, J. & Da Rosa, Á. A. S. U-Pb age constraints on dinosaur rise from south Brazil. *Gondwana Res.* **57**, 133–140 (2018).
19. Müller, R. T. *et al.* Early evolution of sauropodomorphs: Anatomy and phylogenetic relationships of a remarkably well-preserved dinosaur from the Upper Triassic of southern Brazil. *Zool. J. Linn. Soc.* **184**, 1187–1248 (2018).
20. Langer, M. C., McPhee, B. W., de Almeida Marsola, J. C., Roberto-da-Silva, L. & Cabreira, S. F. Anatomy of the dinosaur *Pampadromaeus barberenai* (Saurischia—Sauropodomorpha) from the Late Triassic Santa Maria Formation of southern Brazil. *PLoS ONE* **14**, e0212543 (2019).
21. Pacheco, C. *et al. Gnathovorax cabreirai*: A new early dinosaur and the origin and initial radiation of predatory dinosaurs. *PeerJ* **7**, e7963 (2019).
22. Griffin, C. T. *et al.* Africa's oldest dinosaurs reveal early suppression of dinosaur distribution. *Nature* **609**, 313–319 (2022).
23. Griffin, C. T. & Nesbitt, S. J. The femoral ontogeny and long bone histology of the Middle Triassic (?late Anisian) dinosauriform *Asilisaurus kongwe* and implications for the growth of early dinosaurs. *J. Vert. Paleontol.* **36**, e1111224 (2016).
24. Piechowski, R., Tałanda, M. & Dzik, J. Skeletal variation and ontogeny of the Late Triassic Dinosauriform *Silesaurus opolensis*. *J. Vert. Paleontol.* **34**, 1383–1393 (2014).
25. Brochu, C. A. Closure of neurocentral sutures during crocodilian ontogeny: Implications for maturity assessment in fossil archosaurs. *J. Vert. Paleontol.* **16**, 49–62 (1996).
26. Langer, M. C., Ribeiro, A. M. & Schultz, C. L. The continental tetrapod-bearing Triassic of south Brazil. *N. M. Mus. Nat His. Sci. Bull.* **41**, 201–218 (2007).
27. Wilson, J. A. A nomenclature for vertebral laminae in sauropods and other saurischian dinosaurs. *J. Vert. Paleontol.* **19**, 639–653 (1999).
28. Wilson, J. A., D'Emic, M. D., Ikejiri, T., Moacdieh, E. M. & Whitlock, J. A. A nomenclature for vertebral fossae in sauropods and other saurischian dinosaurs. *PLoS ONE* **6**, e17114 (2011).
29. Wedel, M. J., Cifelli, R. L. & Sanders, R. K. Osteology, paleobiology, and relationships of the sauropod dinosaur *Sauroposeidon*. *Acta Palaeontol. Pol.* **45**(4) (2000).
30. Wedel, M. J. What pneumaticity tells us about "prosauropods", and vice versa. *Spec. Pap. Palaeontol.* **77**, 207–222 (2007).
31. Fedorov, A. *et al.* 3D slicer as an image computing platform for the quantitative imaging network. *Magn. Reson. Imaging* **30**, 1323–1341 (2012).
32. CloudCompare. Version 2.9. 1 [GPL software]. (2018).
33. Aureliano, T. *et al.* Influence of taphonomy on histological evidence for vertebral pneumaticity in an Upper Cretaceous titanosaur from South America. *Cretaceous Res.* **108**, 104337 (2020).
34. Schneider, C. A., Rasband, W. S. & Eliceiri, K. W. NIH Image to ImageJ: 25 years of image analysis. *Nat. Methods* **9**, 671–675 (2012).
35. Woodruff, D., Fowler, D. W. & Horner, J. R. A new multi-faceted framework for deciphering diplodocid ontogeny. *Palaeontol. Electronica* https://doi.org/10.26879/674 (2017).
36. Brum, A. S., Machado, E. B., de Almeida Campos, D. & Kellner, A. W. A. Description of uncommon pneumatic structures of a noasaurid (Theropoda, Dinosauria) cervical vertebra from the Bauru Group (Upper Cretaceous) Brazil. *Cretaceous Res.* **85**, 193–206 (2018).
37. Aureliano, T. *et al.* Exquisite air sac histological traces in a hyperpneumatized nanoid sauropod dinosaur from South America. *Sci. Rep.* **11**, 24207 (2021).
38. Marsh, A. Tutorial 4b: Saurischian vertebral laminae and fossae redux, by Adam Marsh. Sauropod Vertebra Picture of theWeek. https://svpow.com/2015/04/17/tutorial-4b-saurischian-vertebral-laminae-and-fossae-redux-by-adam-marsh/ (2015).Accessed 19th November 2022.
39. Smuts, M. M. The venous drainage of the cervical vertebrae of the ox (Bos taurus L.). *Onderstepoort J. Vet. Res.* **44**, 233–247 (1977).
40. Manning, P. L., Egerton, V. M. & Romano, M. A new sauropod dinosaur from the Middle Jurassic of the United Kingdom. *PLoS ONE* **10**, e0128107 (2015).
41. Taylor, M. & Wedel, M. Why is vertebral pneumaticity in sauropod dinosaurs so variable?. *Qeios* https://doi.org/10.32388/1g6j3q

(2021).

42. Williams, C. J. *et al.* Helically arranged cross struts in azhdarchid pterosaur cervical vertebrae and their biomechanical implications. *iScience* **24**, 102338 (2021).

43. Rolando, M. A., Marsà, J. G. & Novas, F. Histology and pneumaticity of *Aoniraptor libertatem* (Dinosauria, Theropoda), an enigmatic mid-sized megaraptoran from Patagonia. *J. Anat.* **237**, 741–756 (2020).
44. Schwarz, D. & Fritsch, G. Pneumatic structures in the cervical vertebrae of the Late Jurassic Tendaguru sauropods *Brachiosaurus brancai* and *Dicraeosaurus*. *Eclogae Geol. Helv.* **99**, 65–78 (2006).
45. Yates, A. M., Wedel, M. J. & Bonnan, M. F. The Early Evolution of Postcranial Skeletal Pneumaticity in Sauropodomorph Dinosaurs. *Acta Palaeontol. Pol.* **57**, 85–100 (2012).
46. Moore, A. J. Vertebral pneumaticity is correlated with serial variation in vertebral shape in storks. *J. Anat.* **238**, 615–625 (2021).
47. Radermacher, V. J. *et al.* A new *Heterodontosaurus* specimen elucidates the unique ventilatory macroevolution of ornithischian dinosaurs. *Elife* **10**, e66036 (2021).
48. Benson, R. B. J., Butler, R. J., Carrano, M. T. & O'Connor, P. M. Air-filled postcranial bones in theropod dinosaurs: Physiological implications and the "reptile"-bird transition. *Biol. Rev. Camb. Philos. Soc.* **87**, 168–193 (2012).
49. Duncker, H.-R. *The Lung Air Sac System of Birds-a Contribution to the Functional Anatomy of the Respiratory Apparatus* (Springer Berlin Heidelberg, 1971).
50. Wedel, M. J. & Taylor, M. P. Caudal pneumaticity and pneumatic hiatuses in the sauropod dinosaurs Giraffatitan and Apatosaurus. *PLoS ONE* **8**, e78213 (2013).
51. Brum, A. S., Bandeira, K. L. N., Sayão, J. M., Campos, D. A. & Kellner, A. W. A. Microstructure of axial bones of lithostrotian titanosaurs (Neosauropoda: Sauropodomorpha) shows extended fast-growing phase. *Cretaceous Res.* **136**, 105–220 (2022).
52. Gower, D. J. Possible postcranial pneumaticity in the last common ancestor of birds and crocodilians: Evidence from Erythrosuchus and other Mesozoic archosaurs. *Naturwissenschaften* **88**, 119–122 (2001).
53. Bremer, J. L. The pneumatization of the humerus in common fowl and the associated activity of theelin. *Anat. Rec.* https://doi.org/10.1002/ar.1090770209 (1940).
54. Novas, F. E. *et al.* Review of the fossil record of early dinosaurs from South America, and its phylogenetic implications. *J. South Amer. Earth Sci.* **110**, 103341 (2021).

Acknowledgements

The authors would like to thank Adolfo for conducting the microtomography analyses. To the anonymous reviewers, for their contributions to the improvement of the article. Authors' research grants, scholarships, and financial aid were provided by Fundação de Amparo à Pesquisa do Estado de São Paulo (FAPESP 2019/16727-3) 'Taphonomical landscapes' (F.R.B.), Fundação de Amparo à Pesquisa do Estado do Rio Grande do Sul (FAPERGS 1/2551-0002030-0, L.K.; 21/2551-0000619-6, F.A.P.; 21/2551-0000680-3, R.T.M.), and Conselho Nacional de Desenvolvimento Científico e Tecnológico (CNPq grant 307333/2021-3, F.R.B.; CNPq 404095/2021-6. R.T.M.; 422568/2018-0; 309414/2019-9, L.K.).

Author contributions

R.T.M., L.K., F.A.P. collected the specimens. T.A., M.W. worked on the computed tomography. T.A., M.W., A.M.G., M.A.F., F.R.B., R.T.M., L.K., F.A.P analyzed the data and wrote the paper.

Competing interests

The authors declare no competing interests.

Additional information

Supplementary Information The online version contains supplementary material available at https://doi.org/10.1038/s41598-022-25067-8.

Correspondence and requests for materials should be addressed to T.A.

Reprints and permissions information is available at www.nature.com/reprints.

ARTIGO CIENTÍFICO

Aureliano, T., Ghilardi, A.M., Fernandes, M.A., Ricardi-Branco. 2022. Air sac attachments or tendon scars? Distinction between soft tissue traces in the archosaur bone. *Zoological Journal of the Linnean Society*, *in press*.

Status: Manuscrito *in press* na *Zoological Journal of the Linnean Society* (já passou pelo *proof* e será publicado a qualquer momento)

AIR SAC ATTACHMENTS OR TENDON SCARS? DISTINCTION BETWEEN SOFT TISSUE TRACES IN THE ARCHOSAUR BONE

Tito Aureliano[1,2], Aline M. Ghilardi[2], Marcelo A. Fernandes[3], Fresia S. Ricardi-Branco[1]

[1]Institute of Geosciences, University of Campinas. Campinas, Brazil.

[2]Diversity, Ichnology and Osteohistology Laboratory (DINOlab), Department of Geology, Federal University of Rio Grande do Norte. Natal, Brazil.

[3]Laboratory of Paleoecology and Paleoichnology, Federal University of Sao Carlos. Sao Carlos, Brazil.

ABSTRACT

It can be arduous to discriminate between the lamellar bone fibres, the Sharpey's fibres (tendon insertions), and the pneumosteum (air sacs diverticula interaction with the bone) during histological observations. We analysed thin sections of several avemetatarsalians from the Cretaceous of Brazil and brought characters from optical mineralogy to differentiate those biomineralized tissue types, resulting in a solid criterion for histological comparison. The observation scale is one of the best guides to differentiate both tissues. Lamellar bone fibres are only perceptible at very high magnifications (100 X) whilst Sharpey's fibres are detectable at low magnification (5 X). Pneumosteal bone fibres are discernible at 40-50 X. Hence, fibre length is longer in Sharpey's ones than in the pneumosteum. High optical relief is a good proxy to detect connective tissue insertion scars (Sharpey's fibres). Finally, the texture is an excellent proxy to identify pneumosteal bone. The asbestiform aspect of this structure is so far unique among several bone tissue types.

Keywords: pneumosteum - Sharpey's fibres - respiratory system - histology - Sauropoda - Theropoda - Pterosauria - Cretaceous - South America - postcranial skeletal pneumaticity

INTRODUCTION

Archosaurs comprise a diverse and long-lived clade. They adapted to colonize a variety of ecosystems since the Triassic (BRUSATTE; O'CONNOR; JARVIS, 2015; CLAESSENS; O'CONNOR; UNWIN, 2009; FIORILLO; GANGLOFF, 2001; GODOY, 2019; NAVARRO et al., 2022; NESBITT, 2011; PADIAN; WOODWARD, 2021; SOUZA et al., 2021b). One of their

innovations was the postcranial skeletal pneumaticity (BUCHMANN; RODRIGUES, 2019; BUTLER; BARRETT; GOWER, 2012; CERDA; SALGADO; POWELL, 2012; O'CONNOR,

2006; WEDEL, 2006). These pneumatic structures in the skeleton are a reflection of a permeating system of diverticula originating from the lungs which allow for highly effective oxygen-rich unidirectional breathing (LAMBERTZ; BERTOZZO; SANDER, 2018; PROCTOR; LYNCH, 1993; WEDEL, 2003a, 2009; WEDEL; CIFELLI; SANDERS, 2000). This adaptation coevolved with the increased metabolic rates, gigantism, partial thermal regulation, and even flight in saurischian dinosaurs (CERDA et al., 2017; MITCHELL; SANDER, 2014; O'CONNOR, 2004, 2006; PERRY et al., 2009; SANDER et al., 2011b). Structures such as fossae, laminae, and some foramina have been used as evidence of bird-like air sacs attaching to the non-avian dinosaur axial skeleton (O'CONNOR, 2006; TAYLOR; WEDEL, 2021; WEDEL, 2003a, 2007, 2009; WILSON,

2012; WILSON et al., 2011; YATES; WEDEL; BONNAN, 2012). Nonetheless, modern paleontological approaches go beyond macroscopic observations and computed tomography. Histological indicators of this interaction between bone and air sacs diverticula have been reported for some non-avian saurischians and fossil birds (ARANCIAGA ROLANDO; GARCIA MARSÀ; NOVAS, 2020; AURELIANO et al., 2020, 2021b; BRUM et al., 2022; LAMBERTZ; BERTOZZO; SANDER, 2018), although very little is currently known. Consequently, there is a demand to sample more taxa from different phylogenetic contexts, across space and time.

It can often be challenging to distinguish some soft tissue traces in the bone during histological observations. Here we present thin sections of several extinct avemetatarsalians from the Cretaceous of Brazil and establish a solid histological base to discriminate lamellar bone fibres from the Sharpey's fibres (tendon insertions) and the pneumosteum (interaction with air sacs diverticula) in fossil taxa.

MATERIALS AND METHODS

Institutional abbreviations: CPPLIP, Centro de Pesquisas Paleontológicas "Llewellyn Ivor Price", Universidade Federal do Triângulo Mineiro, Uberaba, Brazil; **DINOlab**, Diversity, Ichnology and Osteohistology Laboratory, Departament of Geology, Federal University of Rio Grande do Norte, Natal, Brazil; **DGEO-CTG-UFPE**, Departament of Geology, Centre of Technology and Geosciences, Federal University of Pernambuco, Recife, Brazil; **LPP-UFSCAR**, Laboratory of Paleoecology and Paleoichnology, Federal University of São Carlos, São Carlos, Brazil; **PVL**, Paleovertebrate collection, Instituto "Miguel Lillo", San Miguel de Tucumán, Argentina; **MCT**, Museu de Ciências da Terra, Rio de Janeiro, Brazil; **MPMA**, Museu Paleontológico de Monte Alto, Monte Alto, Brazil.

Material

We analyzed six specimens, including three titanosaurs, two non-avian theropods, and a pterosaur, ranging from the Albian to the Maastrichtian, across Brazil. Table 1 lists all specimens and their context.

Table 1. Specimens selected for the histological analysis in this study.

Taxon	Specimen	Taxonomy	Geological setting	Locality	Age	Sectioning Protocol
Anhangueridae indet.	DGEO-CTG-UFPE 7516	Pterosauria: Pteranodontoidea	Romualdo Formation	Pernambuco, Brazil	Albian	(AURELIANO et al., 2014)
Spinosaurinae indet.	LPP-PV-0042	Saurischia: Theropoda	Romualdo Formation	Ceará, Brazil	Albian	(AURELIANO et al., 2018)
Megaraptora indet.	MPMA 08-003-94	Saurischia: Theropoda	São José do Rio Preto Formation	São Paulo, Brazil	Santonian - Campanian	This work
Ibirania parva	LPP-PV-0200	Saurischia: Sauropoda	São José do Rio Preto Formation	São Paulo, Brazil	Santonian - Campanian	(AURELIANO et al., 2021b)
Arrudatitan maximus	MPMA 12-0001-97-1024	Saurischia: Sauropoda	Adamantina Formation	São Paulo, Brazil	Santonian - Campanian	This work

Uberabatitan ribeiroi	CPPLIP-1024	Saurischia: Sauropoda	Serra da Galga Formation	Minas Gerais, Brazil	Maastrichtian	(AURELIANO et al., 2020)

Anatomical and histological nomenclature

We follow the anatomical nomenclature proposed by Wilson et al. (2011) for vertebral fossae; Wilson (2012) for laminae, and Wedel et al. (2000) and Wedel (2003, 2007) for pneumatic structures. Histological terms, including ‘pneumosteum’ and ‘Sharpey’s fibres’, are in accordance with the standard literature (FRANCILLON-VIELLOT et al., 1990; LAMBERTZ; BERTOZZO; SANDER, 2018; PADIAN; LAMM, 2013; PETERMANN; SANDER, 2013). The terms ‘anterior’ and ‘posterior’ were used instead of cranial and caudal.

Anatomical Abbreviations: General: **c**, centrum; **d**, diapophysis; **fr**, foramen; **pa**, parapophysis; **po**, postzygapophysis; **pr**, prezygapophysis; **s**, neural spine. Laminae: **acdl**, anterior centrodiapophyseal lamina; **cprl**, centroprezygapophyseal lamina; **pcdl**, posterior centrodiapophyseal lamina; **pcpl**, posterior centroparapophyseal lamina; **prpl**, prezygoparapophyseal lamina; **spdl**, spinodiapophyseal lamina; **sprl**, spinoprezygaphoseal lamina. Fossae: **cpaf**, centroparapophyseal fossa; **pacdf**, parapophyseal centrodiapophyseal fossa; **pocdf**, postzygapophyseal centrodiapophyseal fossa; **prpadf**, prezygapophyseal parapodiapophyseal fossa; **prsdf**, prezygapophyseal spinodiapophyseal fossa; **spof**, spinopostzygapophyseal fossa.

Mineralogical description

Mineralogical terms are in accordance with the standard literature (KLEIN; DUTROW, 2007; RAITH; RAASE; REINHARDT, 2011).

Computed tomography

A CT scan of MPMA 12-0001-97-1024 was obtained before histological sampling using a Philips Diamond Select Brilliance CT 16-slice medical scanner with more than 200 slices and a voxel size of 0.75 mm at the Faculty of Medicine, University of São Paulo. Acceleration voltage varied between 90 and 120 kV in a current of 367 mA. The methodology by Aureliano et al. (2020) was followed for data management and generating three-dimensional reconstruction with the software *3D Slicer* v. 4.10 (FEDOROV et al., 2012) and *CloudCompare* 2.9.1 (CLOUDCOMPARE, 2018). CT scan results are in Supporting Information. Tomography data was uploaded to the Morphobank platform and is available through this link: http://morphobank.org/permalink/?P4403.

Bone histology

The main objective of histological sampling was to detect and describe the presence of ‘pneumosteal bone’. Pneumosteum is a peculiar type of secondary bone similar to ‘tiny hair-like structures’ which correlates with postcranial skeletal pneumaticity and, thus, to the lungs and their diverticula (LAMBERTZ; BERTOZZO; SANDER, 2018). All thin sections are housed at the DINOlab. Some were previously processed and qualitatively described in other publications are further utilized here to quantify morphological characters (see Table 1 for references). For the methodology applied in specimens DGEO-CTG-UFPE 7516, LPP-PV-0042, LPP-PV-0200, and CPPLIP-1024, see their respective references also in Table 1. Pneumatic air sacs are hypothesized to penetrate the fossil bone throughout deep vertebral fossae delimited by well-defined laminae.

To test for the presence of pneumosteum in *Arrudatitan maximus* Silva Junior, Martinelli, Iori, Marinho, Hechenleitner, and Langer, 2022 (MPMA 12-0001-97; Santucci *et al.*, 2011), we cross-sectioned the acdl and the pcdl of the neural arch. Additionally, we experimentally sampled the surface of the prezygapophysis for histological control in an area with complex connections with tendons where pneumosteum was not expected (see Figure S1 in Supporting Information for the planes of the section). Sections across the laminae of MPMA 12-0001-97 were produced following standard procedures (LAMM, 2013b; LAMM; PADIAN, 2013). The thin section of the megaraptoran MPMA 08-003-94 centrum wall was taken with this same procedure. The prezygapophysis sample of MPMA 12-0001-97 was obtained from a core drill (STEIN; SANDER, 2009). The samples were pruned to a thickness of ~40-50 µm. For MPMA 12-0001-97, LPP-PV-0200, and CPPLIP-1024, thin sections were observed and photographed by using a petrographic ZEISS Axioscope microscope with an AxioCam MRc 5 camera attached and imaging software ZEISS Application Suite v. 4.4. The rest of the specimens were analyzed in a Leica DM750P microscope with adaptors connected with a Canon Rebel T5i camera. Pictures were corrected for brightness and contrast in Adobe Photoshop CC 20.0.1, and composite images were prepared in Corel Draw X6. Photomicrographs of lamellar bone fibres, Sharpey's fibres and pneumosteum are represented in Figures 1, 2 and 3, respectively. Figure 4 demonstrates the distinct magnification properties of these three tissues side-by-side.

RESULTS

Comparative histological data for extinct avemetatarsalian taxa

Pterosauria: Pteranodontoidea: Anhangueridae indet.. DGEO-CTG-UFPE 7516, ulna (AURELIANO et al., 2014).

The ulna of a large pterodactyloid pterosaur is nearly complete and only misses the proximal epiphysis. The midshaft cross-section histological profile indicates an adult individual as evidenced by the presence of an External Fundamental System (EFS). There is a broad medullary cavity and foramina were absent. Primary lamellar bone dominates (Figure 1A-F). No Sharpey's fibres were detected.

Saurischia: Theropoda: Spinosaurinae indet.. LPP-PV-0042, tibia (AURELIANO et al., 2018).

The fragmentary tibia of a large Spinosaurinae presents a pachyosteosclerotic condition. The cross-section at the distal-most slice of the metaphysis indicates a growing subadult. This is supported by the absence of an EFS, prevalence of plexiform vascularization and limited presence of secondary osteons in the outer cortex. Lamellar bone populates the cortex and secondary osteons are present in the periosteum (Figure 1G-L). There are long Sharpey's fibres medially and 'cross pattern' ones posteriorly (Figure 2G-I).

Saurischia: Theropoda: Megaraptora indet.. MPMA 08-003-94, anterior caudal vertebra (MENDÉZ; NOVAS; IORI, 2012).

The caudal vertebra is fragmentary and only preserves the centrum. Large pneumatic cavities (pneumatopores) carve each surface of the centrum laterally and present a rugose texture. A thin section extracted dorsally above this pneumatic structure shows thin trabecular walls and camellate tissue is composed of pneumosteum (Figure 3A-C).

Saurischia: Sauropoda: Titanosauria: *Ibirania parva* Navarro, Ghilardi, Aureliano, Díaz, Bandeira, Cattaruzzi, Iori, Martine, Carvalho, Anelli, Fernandes, Zaher, 2022. LPP-PV-0200, dorsal vertebra (AURELIANO et al., 2021b).

The vertebra of this adult nanoid sauropod is nearly complete. It shows many features of invasive pneumatization, including deep fossae and well-defined laminae. The cross-section of the centrum reveals an arrangement of tiny trabeculae structuring the internal pneumatic camellae (pneumosteum; Figure 3G-I). Pneumosteal bone fibres appear at higher magnification (40x; Figure 3I).

Saurischia: Sauropoda: Titanosauria: *Uberabatitan ribeiroi* Salgado & Carvalho, 2008. CPPLIP-1024, cervical vertebra (AURELIANO et al., 2020; SALGADO; CARVALHO, 2008; SILVA JUNIOR et al., 2019).

The posterior portion of the neural arch is fragmentary but the anterior part is well preserved. There are deep fossae and well-defined laminae. CT scan slices demonstrate a complex architecture of thin camellate tissue. A cross-section of the prezygapophysis reveals that camellae comprehend pneumosteal bone tissue (Figure 3D-F). No Sharpey's fibres were detected.

Saurischia: Sauropoda: Titanosauria: *Arrudatitan maximus* Santucci & Arruda-Campos, 2008 (Silva Junior, Martinelli, Iori, Marinho, Hechenleitner, Langer, 2022). MPMA 12-0001-97-1024, dorsal vertebra (SANTUCCI; ARRUDA-CAMPOS, 2011; SILVA JUNIOR et al., 2022). See supplemental information.

The vertebra is considerably fragmentary. Several parts are badly preserved and have collapsed during early burial or diagenesis, probably due to the highly pneumatized nature of the bone. There are some anatomical observations missing in the literature worth mentioning below.

The anterior-most portion of the neural arch is slightly eroded in lateral view and very compromised in proximal view (>50% loss of material). Only the left lateral portion has been preserved. Foramina are absent throughout the preserved volume but the sedimentary matrix still covers most fossae. The diapophysis has collapsed but can be identified. Part of the vertebral centrum is preserved but has been mistakenly identified as the prezygapophysis by Santucci & Arruda-Campos (2011). The prezygapophysis has been deformed by a smooth proximal twist. The prezygapophysis has a subcircular articulation, sizeable and convex. The parapophysis is dislocated anteriorly towards the centrum and bears a thick and flat articular facet that connects to the latter. It is surrounded by two deep fossae (cpaf and prpadf) and is connected to three laminae (cprl, prpl and acdl). A further two laminae (pcpl and pcdl) connect to the mid-posterior portion of the centrum. The fossae prpadf, cpaf, and pocdf are very deep, but pacdf is subtle and partially covered by collapsed bone. The neural spine is more abraded than the region between the diapophysis and the centrum. However, traces of collapsed laminae (spdl and sprl) and two fossae (prsdf and spof) can be detected. The dorsal vertebra MPMA 12-0001-97-1024 shows an advanced degree of complexity and leads us to conclude it was placed more posteriorly than originally proposed by Santucci & Arruda-Campos (2011). CT scan did not reveal much about the internal structures due to diagenetic artefacts (see Supporting Information for more details).

Finally, cross-sections of the laminae (pcdl and acdl) and the core section of the prezygapophysis reveal lamellar bone throughout the cortex. There are neither trabeculae nor pneumosteum. There are many traces of Sharpey's fibres, which is expected in an area with complex morphology with many muscles and tendons (Figure 2).

Observations on tissue optical properties

Lamellar bone fibres are very short and only detectable at very high magnifications (>100X; Figure 1). They present low to average optical relief and extinction may be undulose or absent. Fibres present parallel or inclined patterns. Pneumosteum is distinguished from regular trabeculae by an array of tiny asbestiform densely-packed fibres, usually shorter than 60 µm (Figure 3C,F,I). These fibres feature low relief and undulose extinction. Sharpey's fibres are larger, show higher optical relief (*sensu* Klein & Dutrow, 2007), and have greater lengths when directly compared to pneumosteal fibres. They may also show high birefringence with lambda compensator and therefore help the observer detect such structures at lower magnifications (Figure 2G,I). The main highlights of these structures are the high optical relief, undulose extinction, and insertion angles of approximately 60° (Figure 2). Each of these fibres is much longer (>200 µm) and wider than the pneumosteum packs (<60 µm). Sharpey's fibres also exhibit an organized parallel pattern in contrast to the chaotic asbestiform organization of the pneumosteal fibres. A list discerning the optical features between different fibres is presented in Table 2.

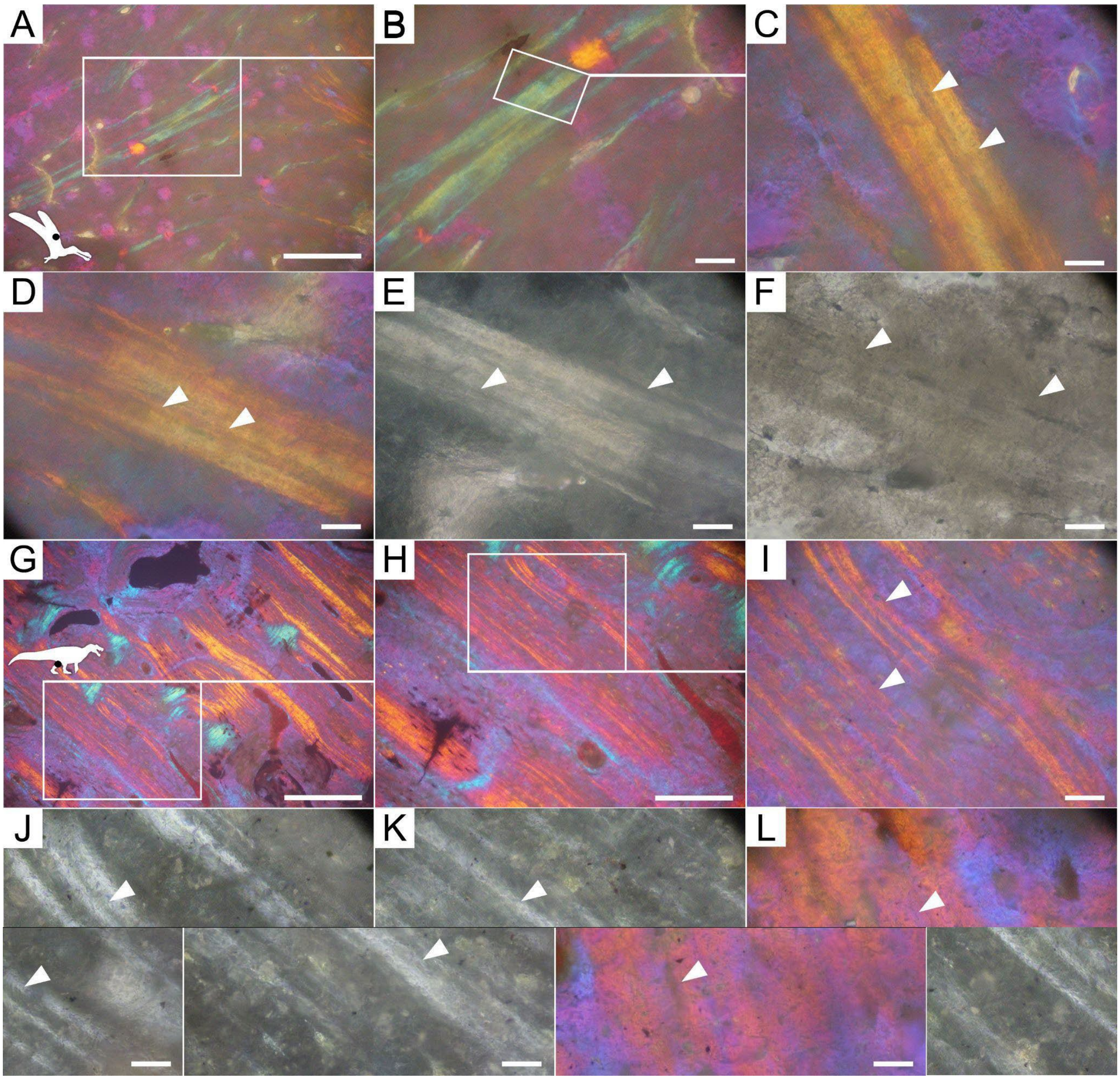

Figure 1. Lamellar bone fibres in an anhanguerid pterosaur ulna (DGEO-CTG-UFPE 7516; A-F) and in a spinosaurine theropod tibia (LPP-PV-0042; G-L). Note that these fibres are only visible at very high magnifications (100X; arrow). Silhouettes in **A** and **G** indicate sampled elements (not to scale; art by Felipe A. Elias). All polarized light. Crossed nicols in A-E and G-L. Compensator in A-D, G-I, and L. Parallel nicols in F. The relative angle to the cortical surface is approximately 80º in A-B; 340º in C; 290º in D-F; 120º in G-L. Scale bar in A,H = 250 µm; in B,I = 50 µm; G = 500 µm; in C-F, J-L = 10 µm.

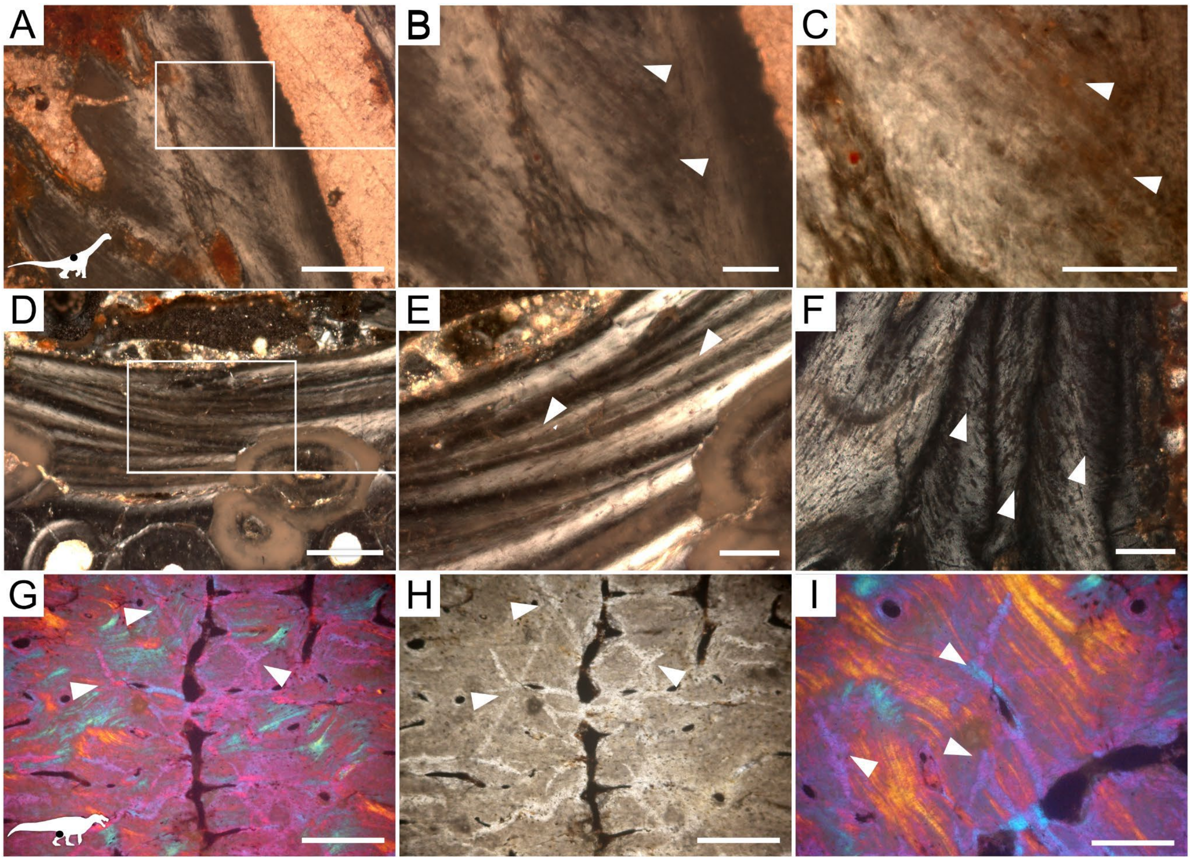

Figure 2. Sharpey's fibres in a dorsal vertebra of *Arrudatitan* (MPMA 12-0001-97-1024; A-F) and in a spinosaurine theropod tibia (LPP-PV-0042; G-I). Note that these fibres are visible at low magnifications (5X; arrow). G-H show a cross pattern of Sharpey's fibres. Silhouettes in **A** and **G** indicate sampled elements (not to scale; art by Felipe A. Elias). All polarized light. Crossed nicols in A-F. Compensator in G, H. Parallel nicols in H. The relative angle to the bone surface is approximately 150º in A-C; 90º in D; 70º in E; 120º in F; 90º in G-I. Scale bar in A = 300 µm; in D,I = 250 µm; in B,C,E,F = 100 µm; G,H = 500 µm.

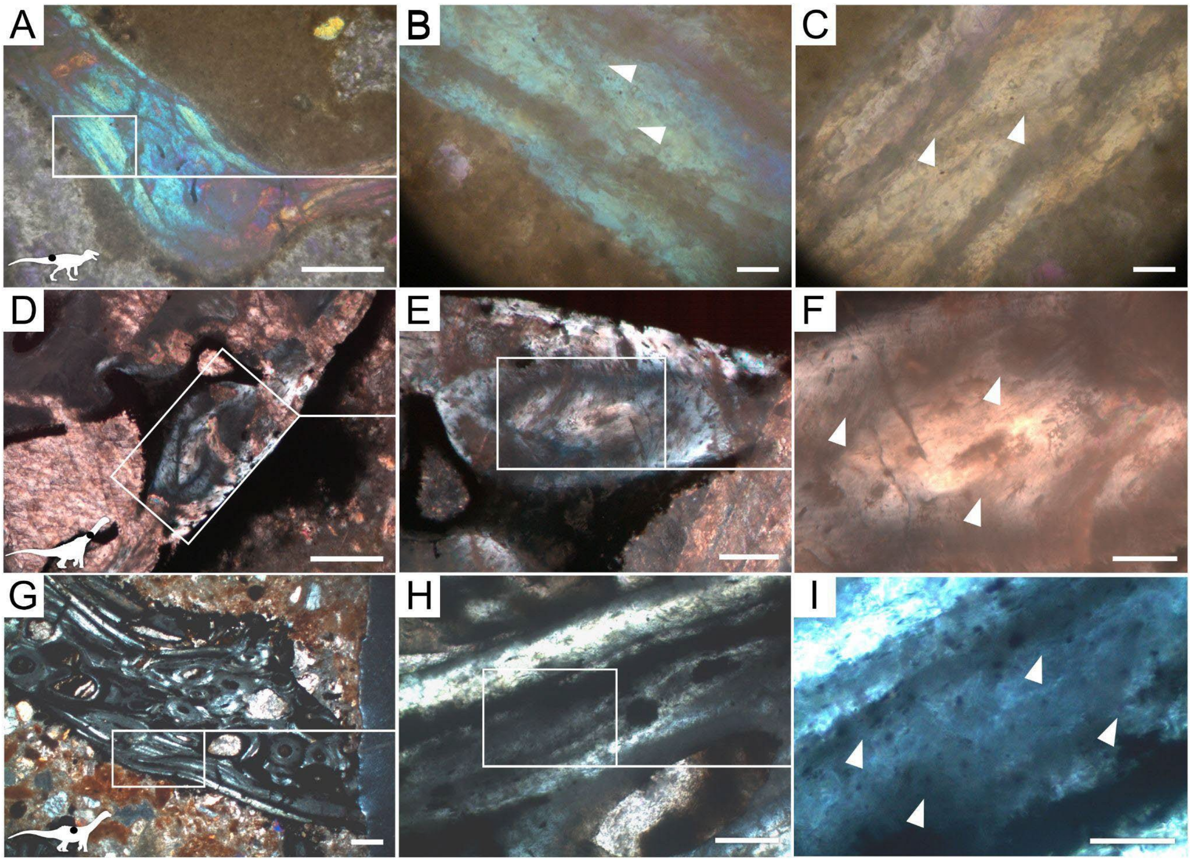

Figure 3. Pneumosteum in saurischian dinosaurs. **A-C**, a megaraptoran theropod caudal vertebra (MPMA 08-003-94). **D-F**, a cervical vertebra of the lithostrotian titanosaur *Uberabatitan* (CPPLIP-1024). **G-I**, a dorsal vertebra of a saltasaurid titanosaur *Ibirania* (LPP-PV-0200). Pneumosteum is distinguished from regular lamellar bone for comprising an array of tiny asbestiform densely packed fibres (usually shorter than 60 µm; arrow). These feature low optical relief and undulose extinction. Silhouettes in A, D, and G indicate sampled elements (not to scale; art by Felipe A. Elias). All polarized light. Crossed nicols in A-E and G-L. Compensator in A-D, G-I, and L. Parallel nicols in F. The relative angle to the bone surface is approximately 320º in A-B; 220º in C-D; 105º in E-F; 290º in G; 80º in H-I. Scale bar in A,D = 250 µm; in C,E = 100 µm; B,F,H,I = 50 µm; in G = 200 µm.

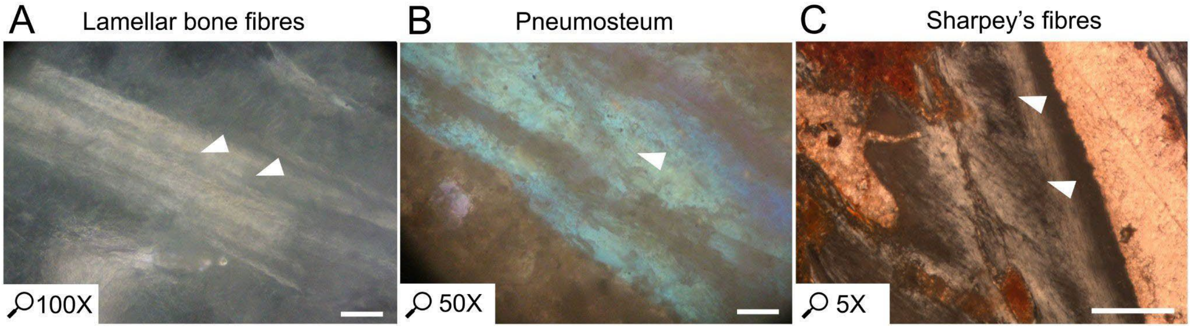

Figure 4. Side-by-side comparison plate between lamellar bone fibres (**A**), pneumosteum (**B**), and the Sharpey's fibres (**C**), all indicated by arrows. **A**, an anhanguerid pterosaur ulna (DGEO-CTG-UFPE 7516). **B**, a megaraptoran theropod caudal vertebra (MPMA 08-003-94). **C**, a dorsal vertebra of *Arrudatitan* (MPMA 12-0001-97-1024). Magnifier indicates microscope

magnification. All polarized light and crossed nicols. Compensator in B. Parallel nicols in F. The relative angle to the bone surface is approximately 290º in A; 320º in B; 150º in C. Scale bar in A = 10 µm; in B = 50 µm; in C = 300 µm.

Table 2. Distinct optical mineralogical properties between lamellar bone fibres, pneumosteum, and Sharpey's fibres.

Tissue	**Minimum magnification required**	**Fibre length**	**Optical relief**	**Extinction**	**Texture / Pattern**
Pneumosteum	40 X	usually shorter than 60 µm	low	always undulose	asbestiform (chaotic)
Sharpey's fibres	5 X	usually longer than 200 µm	high	may be undulose or absent	inclined parallel lines at specific angles (eg. 60º)
Lamellar bone fibres	100 X	very short	low to average	may be undulose or absent	parallel and inclined lines

DISCUSSION

New insights on the pneumosteum

The evolution of pneumatic structures played a definitive role in archosaur phylogeny (BUTLER; BARRETT; GOWER, 2009, 2012; CLAESSENS; O'CONNOR; UNWIN, 2009; O'CONNOR, 2006; WEDEL, 2006, 2007). Classically, the association between the skeleton and the respiratory system has been limited to macroscopic observations and tomographies (CERDA; SALGADO; POWELL, 2012; WILSON, 2012; WILSON et al., 2011; YATES; WEDEL; BONNAN, 2012). Fortunately, it is also possible to investigate the histology of the air sacs diverticula interaction with the skeleton throughout the identification of a specific secondary bone tissue called pneumosteum (LAMBERTZ; BERTOZZO; SANDER, 2018). This tissue has been reported for very few taxa, however. The pneumosteal bone in the analyzed specimens has confirmed several characteristics found in previous studies (AURELIANO et al., 2020; LAMBERTZ; BERTOZZO; SANDER, 2018). Additionally, we now advance the criteria for the description of this tissue by applying descriptive concepts from optical mineralogy in this study.

It may be quite challenging to distinguish pneumosteum from lamellar bone fibres, and from the ones resulting from muscle and tendon insertions (Sharpey's fibres). We established a solid base for histological comparison between these tissues (see Table 2). All Sharpey's fibres found in this approach are in accordance with previous observations from other taxa (PEREYRA et al., 2019; PETERMANN; SANDER, 2013; SANCHEZ et al., 2013). We observed that they exhibit a high relief, undulose extinction, and insertion angles of approximately 60° relative to the cortical surface. It is also known in the literature that these insertion angles are variable according to the muscular system associated with them (PETERMANN; SANDER, 2013). These fibres are considerably longer (>200 µm) and thicker (<60 µm) than both the pneumosteum and the lamellar bone ones. Another difference is that the former shows an organized parallel pattern in contrast to the chaotic asbestiform organization of the latter.

We now have data for a broad comparison to distinguish these three tissue types in the fossil record. The next steps for future research should be to expand the sampling of modern taxa to test whether the same properties are observable in non-fossilized contexts.

CONCLUSIONS

We established a solid base for the histological comparison to distinguish pneumosteum from the lamellar bone fibres and Sharpey's fibres within fossil avemetatarsalians. Selected highlights are listed below:

- The inspection scale is one of the best guides to differentiate both tissues. Lamellar bone fibres are only observable at very high magnifications (100 X) whilst Sharpey's fibres are detectable at low magnification (5 X). Pneumosteal bone fibres are discernible at 40-50 X. Consequently, fibre length is longer in Sharpey's ones than in the pneumosteum.
- High optical relief is a good proxy to detect connective tissue insertion scars (Sharpey's fibres).
- Texture is a good proxy to identify pneumosteal bone. The asbestiform aspect of this structure is so far unique among several bone tissue types.

Our results will assist colleagues in collecting more data to expand the knowledge on the evolution of the respiratory system in archosaurs.

ACKNOWLEDGEMENTS

We would like to acknowledge Paulo Saldiva and the rest of the USP Faculty of Medicine team for conducting fossil tomography. To Martin Sander and anonymous reviewers, for commenting on an earlier version of the manuscript. To Sandra Tavares and Fabiano Iori for their assistance at the Monte Alto Paleontological Museum collection and for allowing the sampling. To the Departamento de Pós-Graduação do Instituto de Geociências, Unicamp, and to *Bone Collectors Studio*, for funding transportation and some thin sections. Authors' research grants, scholarships, and financial aid were provided by the Brazilian National Council for Scientific and Technological Development (CNPq 131.777/2018-1 and 307333/2021-3) (T.A.), the Brazilian Coordination for the Improvement of Higher Education Personnel (CAPES - Finance Code 001) (A.M.G), and FAPESP 2016/20927-0 'Modern accumulation studies and fossil bioclast studies in continental and coastal environments' (F.R.B.).

Supplementary material: Observations and Analysis on *Arrudatitan maximus*

MATERIAL

Specimen: MPMA 12-0001-97-1024 (neural arch of a posterior dorsal vertebra). The specimen is part of the holotype of *Arrudatitan maximus* Santucci & Arruda-Campus (2011). Features of other elements of this specimen indicate this was an adult individual (SANTUCCI; ARRUDA-CAMPOS, 2011). However, no skeletochronological histology has been published so far.

Locality and horizon: Monte Alto municipality, São Paulo State, Turonian-Santonian Adamantina Formation (CASTRO et al., 2018; SANTUCCI; ARRUDA-CAMPOS, 2011), Bauru Group, Southeast Brazil.

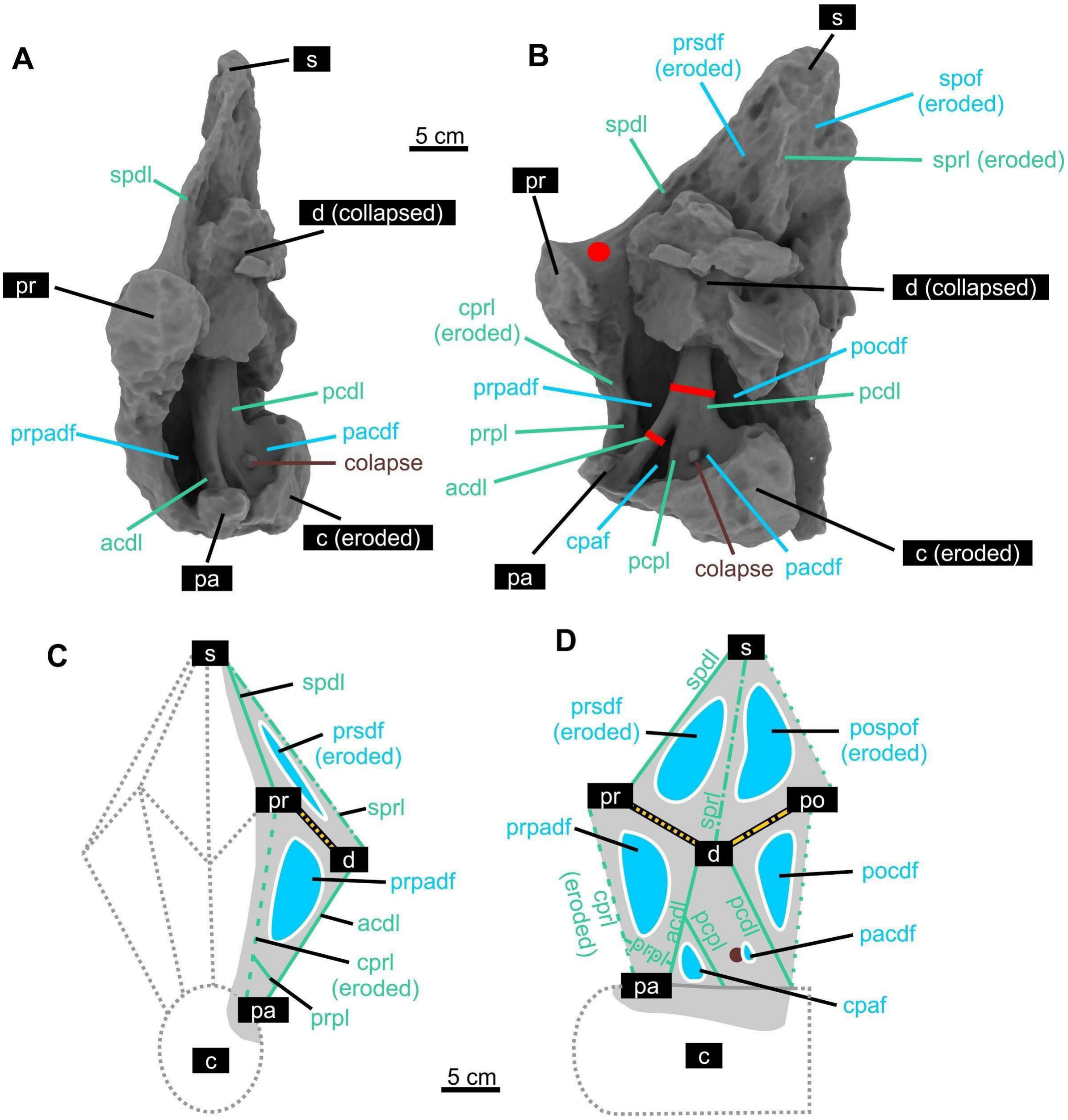

Figure S1. Neural arch of a posterior dorsal vertebra of the Late Cretaceous Brazilian titanosaur *Arrudatitan maximus* (MPMA 12-0001-97-1024). Three-dimensional reconstruction from CT scan (A, B) and schematic morphological diagrams (C, D) in anterior (A, C) and left lateral (B, D) views. Red lines and dots show sampling planes. **Abbreviations:** **acdl**, anterior centrodiapophyseal lamina; **c**, centrum; **cpaf**, centroparapophyseal fossa; **cprl**, centroprezygapophyseal lamina; **d**, diapophysis; **pacdf**, parapophyseal centrodiapophyseal fossa; **pa**, paraphophysis; **pcdl**, posterior centrodiapophyseal lamina; **pcpl**, posterior centroparapophyseal lamina; **po**, postzygapophysis; **pocdf**, postzygapophyseal centrodiapophyseal fossa; **pr**, prezygapophysis; **prpl**, prezygoparapophyseal lamina; **prpadf**, prezygapophyseal parapodiapophyseal fossa; **prsdf**, prezygapophyseal spinodiapophyseal fossa; **s**, neural spine; **spdl**, spinodiapophyseal lamina; **spof**, spinopostzygapophyseal fossa; **sprl**, spinoprezygaphoseal lamina.

RESULTS

CT scanning of neural arch MPMA 12-0001-97-1024

The tomography slices allowed a 3D reconstruction of the *Arrudatitan* neural arch MPMA 12-0001-97-1024. However, internal preservation was too poor, and artefacts abound in the images throughout the neural arch (Fig.2.A.1-3). These might be the reasons why most of the internal pneumatic structures could not be assessed through the tomographic images. However, the CT scans show that there is an array of elongated cavities arranged in parallel extending from the prezygapophysis to the neural spine throughout the spdl. Camellae are smaller at the prezygapophysis and the spdl (average diameter = 2.4 mm) but increase towards the neural spine (average diameter = 5.9 mm). The prezygapophysis shows a subcircular camellate architecture in proximal view which projects radially towards the spdl (Fig.2.3). The laminae pcdl and acdl (Fig.2.1-3) showed a continuum of uniform lower density along their long axis. The preserved portion of the vertebral centrum showed no pneumatic bone structures most possibly due to diagenetic deformation.

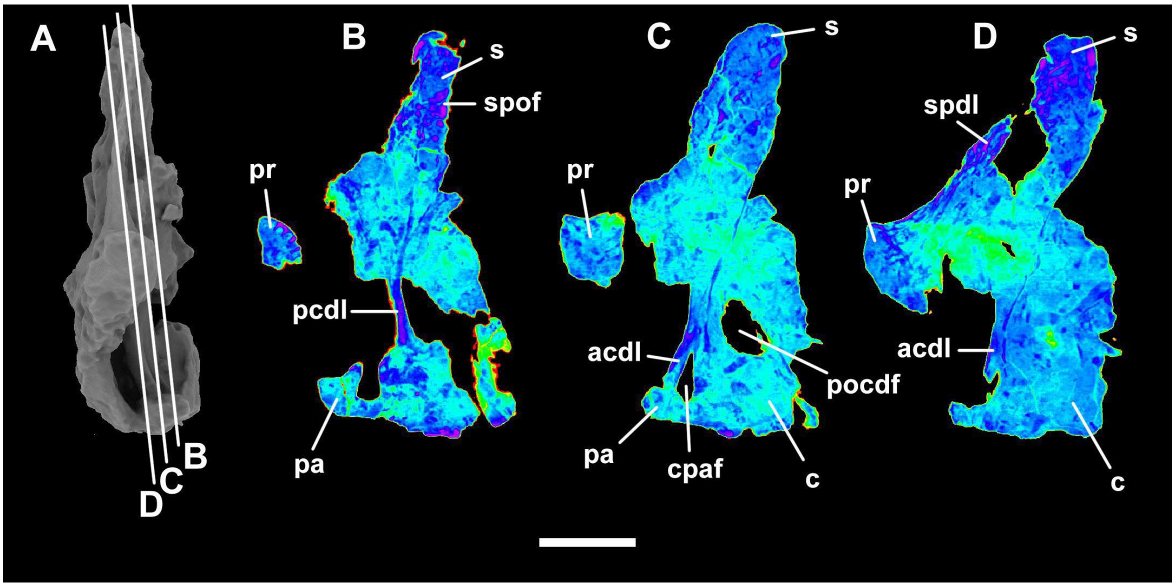

Figure S2. Internal structures of the dorsal neural arch of MPMA 12-0001-97-1024. **A**, 3D surface model in proximal view illustrating the location of three subvertical tangential virtual sections (B-D). Virtual sections with density are plotted in false colour. Purple and darker blue indicate areas of lower density (i.e., pneumatic cavities). The lighter blue and green indicate denser structures (i.e., bone walls). The sections show that only a few pneumatic structures survived taphonomic processes. In this particular case, the green colours might also indicate sediment infill and imaging artefacts. **Abbreviations: acdl**, anterior centrodiapophyseal lamina; **c**, centrum; **cpaf**, centroparapophyseal fossa; **pa**, paraphophysis; **pcdl**, posterior centrodiapophyseal lamina; **pocdf**, postzygapophyseal centrodiapophyseal fossa; **pr**, prezygapophysis; **spdl**, spinodiapophyseal lamina; **spof**, spinopostzygapophyseal fossa. Scale bar = 10 cm.

Taphonomy and petrography

The neural arch preserves only its left lateral mid-anterior region. The specimen shows evidence of mechanical abrasion and bone collapse that occurred before or soon after embedding with sediments. There are abraded osteons on the surface indicating pre-burial mechanical transportation (Figure S3A). Empty spaces and the concave bottom surface of the laminae were filled by clastic sediment (Figure S3). These mostly comprise mineral grains of quartz, K-feldspar, and clay. Very poorly sorted angular to subrounded grains abound (Figure S3B). Originally open spaces are also filled in by bone fragments originating from collapsed trabeculae (see supplementary material). Late diagenesis alteration is substantiated by microcracks throughout the trabeculae (Figure S3A, C). Post- exhumation weathering signs are validated by the presence of opaque oxide minerals infilling the secondary osteons centripetally (PFRETZSCHNER, 2004) (Figure S3D). Nonetheless, the microanatomy is well-preserved to the microscopic level and histology could be accessed. The fact that the bone is birefringent in cross-polarized light indicates good preservation of the bone apatite.

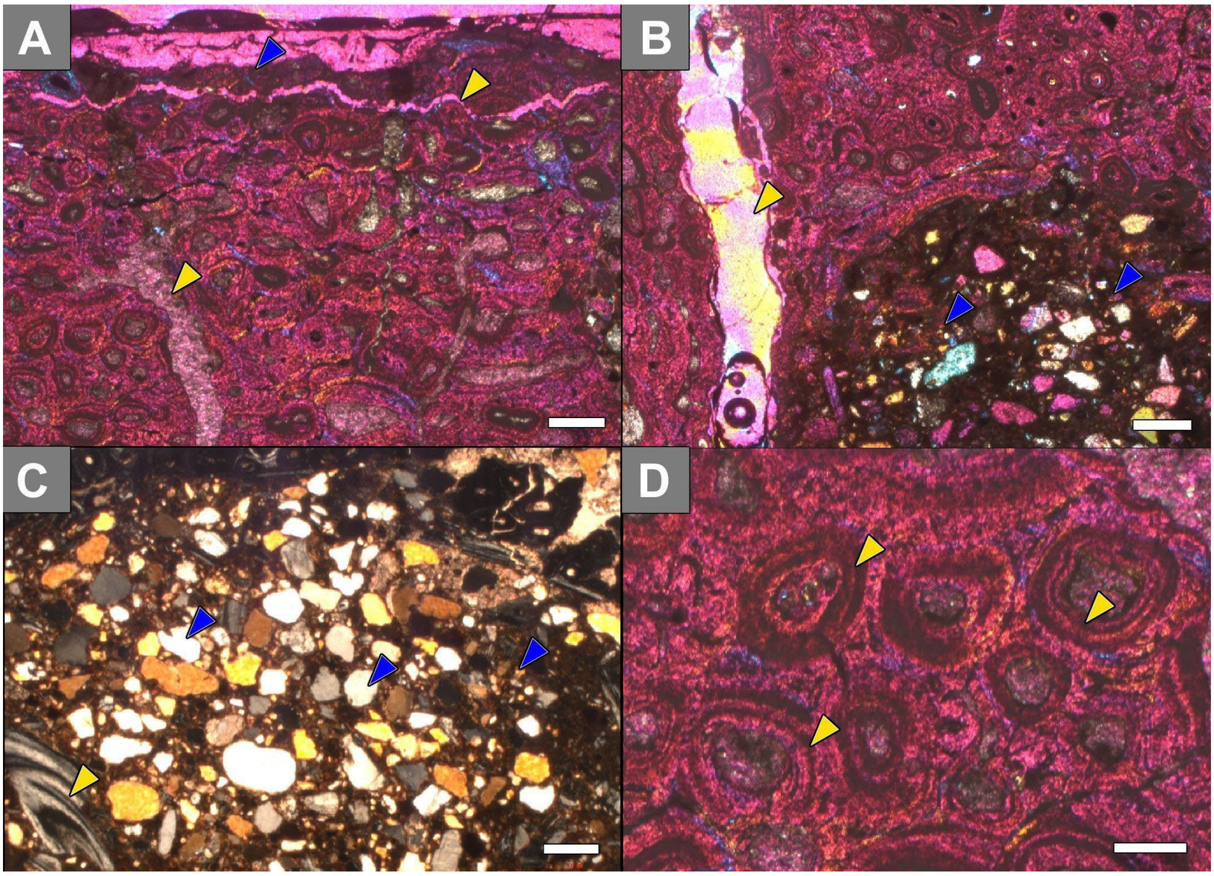

Figure S3. The taphonomy of MPMA 12-0001-97-1024 in thin sections. **A**, abraded osteons at the surface (dark blue arrow) and microcracks in the trabeculae (light yellow arrows). **B**, late diagenetic fracture crossing the trabeculae of pcpl (light yellow arrow), and clastic sedimentary grains in contact with the internal surface of the lamina (dark blue arrow). **C**, very poorly sorted subrounded to angular mineral grains (blue arrow) and fragments of collapsed bone trabeculae (yellow arrow) amidst the sedimentary matrix. Note the well-preserved birefringence of the bone apatite crystallites. The unusually high quartz and feldspar birefringence was caused because by thin sections being thicker than the petrographic standard (> 32 µm). D, opaque oxide minerals infilled the lamellar bone in secondary osteons centripetally (arrows) during weathering. Cross-polarized light in **A-D** with the lambda compensator in **A**, **B**, **D**. Scale bar in **A, B, C** = 500 µm; in **D** = 200 µm.

DISCUSSION

Redescription of the neural arch of *Arrudatitan maximus*

The original description of MPMA 12-0001-97-1024 by Santucci & Arruda-Campos (2011) has mistakenly identified the centrum as the prezygapophysis. Consequently, the latter has been wrongly identified as the diapophysis. However, the actual diapophysis was destroyed during diagenesis. Furthermore, the complexity of the laminae/fossae arrangement indicates the specimen is a posterior dorsal vertebra (WILSON, 2012; WILSON et al., 2011) instead of an anterior one (contra Santucci & Arruda-Campos, 2011).

Pneumatic macroscopic structures in *Arrudatitan maximus*

Despite the extensive diagenetic destruction, several pneumatic structures in a neural arch of the *Arrudatitan maximus* holotype are preserved and associated with the organism's respiratory system. A complex arrangement between fossae and laminae once gave support to pulmonary diverticula. The acdl and pcdl laminae contain no camellae, but there is a single foramen in their fused table. CT scan images showed that the specimen was diagenetically compromised and few data could be extracted from the images. Nonetheless, they reveal a camellate architecture in the neural arch, spdl, spof, and in the prezygapophysis. These internal pneumatic cavities are elongated between the prezygapophysis and the neural spine, and slightly radial to the prezygapophysis articulation surface. A similar pattern has been observed in the cervical cotyles of *Austroposeidon magnificus* MCT 1628-R (BANDEIRA et al., 2016) and *Uberabatitan ribeiroi* CPPLIP-1024 (AURELIANO et al., 2020). Therefore, this pattern may correlate to the structural needs of the vertebral articulation surfaces instead of being restricted to any specialized area. Elongated cylindrical bone walls perpendicular to the surfaces may have been a histological adaptation to sustain axial mechanical stresses (CHRISTIAN; DZEMSKI, 2011; HOHN, 2011; PADIAN et al., 2013). The neural spinal camellate fabric of MPMA 12-0001-97-1024 shows no continuous shape and size. The architecture of the latter could not be directly compared to *Saltasaurus loricatus* (CERDA; SALGADO; POWELL, 2012), *Austroposeidon magnificus* (BANDEIRA et al., 2016), and *Uberabatitan ribeiroi* (AURELIANO et al., 2020) because of lack of CT data.

ARTIGO CIENTÍFICO

Aureliano, T., Ghilardi, A.M., Fernandes, M.A., Ricardi-Branco. 2022. The origins of na invasive air sac system in sauropodomorph dinosaurs. *The Anatomical Record*, submetido.

Status: Manuscrito submetido para *The Anatomical Record*

THE ORIGIN OF AN INVASIVE AIR SAC SYSTEM IN SAUROPODOMORPH DINOSAURS

Tito Aureliano[1,2,5*], Aline M. Ghilardi[2], Rodrigo T. Müller[3,4], Leonardo Kerber[3,4], Marcelo A. Fernandes[5], Fresia Ricardi-Branco[1], Mathew J. Wedel[6]

[1]Institute of Geosciences, University of Campinas (Unicamp). Campinas, Brazil.

[2]Diversity, Ichnology and Osteohistology Laboratory (DINOlab), Department of Geology, Federal University of Rio Grande do Norte (URFN). Natal, Brazil.

[3]Centro de Apoio à Pesquisa Paleontológica da Quarta Colônia (CAPPA), Federal University of Santa Maria (CAPPA/UFSM). São João do Polêsine, Brazil.

[4]Programa de Pós-Graduação em Biodiversidade Animal, Federal University of Santa Maria (UFSM). Santa Maria, Brazil.

[5]Laboratório de Paleoecologia e Paleoicnologia (LPP), Departamento de Ecologia e Biologia Evolutiva (DEBE), Federal University of São Carlos (UFSCar). São Carlos, Brazil.

[6]College of Osteopathic Medicine of the Pacific and College of Podiatric Medicine, Western University of Health Sciences. Pomona, United States of America.

*Corresponding author

ABSTRACT

One of the most remarkable features in sauropod dinosaurs relate to their pneumatized skeletons permeated by a bird-like air sac system. Many studies described the late evolution and diversification of this trait in mid to late Mesozoic forms but few focused on the origin of the invasive respiratory diverticula in sauropodomorphs. Fortunately, it is possible to solve this thanks to the boom of new species described in the last decade as well as the broad accessibility of new technologies. Here we analyze the unaysaurid sauropodomorph *Macrocollum itaquii* from the Late Triassic (early Norian) of southern Brazil using micro-computed tomography. We describe the chronologically oldest and phylogenetically earliest unambiguous evidence of an invasive air sac system in a dinosaur. Surprisingly, this organism presented a unique pattern of pneumatization in non-sauropod sauropodomorphs, with pneumatic foramina in posterior cervical and anterior dorsal vertebrae. This suggests that patterns of pneumatization were not cladistically consistent prior to the arrival of Jurassic eusauropods. Additionally, we describe the protocamerae tissue, a new type of pneumatic tissue with properties of both camellae and camerae. This reverts the previous hypothesis which stated that the skeletal pneumatization first evolved into camarae, and derived into delicate trabecular arrangements. This tissue is evidence of thin camellate-like tissue developing into larger chambers. Finally, Macrocollum is an example of the gradual evolution of skeletal tissues responding to the fastly specializing Respiratory System of saurischian dinosaurs.

Keywords: respiratory system, Ornithodira, bone histology, Triassic, South America

INTRODUCTION

Sauropods were an emblematic clade of long-necked dinosaurs that colonized all continents during the Jurassic and Cretaceous (CERDA et al., 2012; CURRY ROGERS; FORSTER, 2001; DÍEZ DÍAZ, 2022; GHILARDI et al., 2016; MO et al., 2022; RIGBY et al., 2021; WIERSMA-WEYAND et al., 2021). Some lineages attained gigantic scales turning these the largest animals out of the oceans (CARBALLIDO et al., 2017; GONZÁLEZ RIGA et al., 2016; LACOVARA et al., 2014; OTERO et al., 2021). One of the features that allowed the body enlargement was a structural decrease of density caused by the presence of a bird-like air sac system (PERRY et al., 2009; SANDER et al., 2011). The identification of a Postcranial Skeletal

Pneumaticity (PSP) is the current method to identify the diverticular respiratory system in fossil taxa (BRITT, 1994). The evaluation of unambiguous PSP requires the identification of deep vertebral fossae containing foramina connecting with internal pneumatic structures such as camerae and camellae (O'CONNOR, 2006). The unambiguous PSP has been extensively reported in neosauropods, especially titanosauriforms (BANDEIRA et al., 2016; CERDA; SALGADO; POWELL, 2012; SCHWARZ; FRITSCH, 2006; WEDEL, 2003; WEDEL; CIFELLI; SANDERS, 2000; WOODWARD; LEHMAN, 2009; ZURRIAGUZ; POWELL, 2015). Contrastingly, few studies focused on the origins of these diverticula in the clade, and much of the knowledge on non-sauropod sauropodomorphs remains with scarce evidence (BUTLER; BARRETT; GOWER, 2012; WEDEL, 2007, 2009; YATES; WEDEL; BONNAN, 2012). The recent evidence showing the absence of PSP in the earliest dinosaurs (AURELIANO et al., 2022) suggested this trait was not homologous in ornithodirans and that invasive air sacs evolved at least three times independently, in theropods, sauropodomorphs, and pterosaurs. This discovery raised a demand to investigate how and when these structures emerged during the Late Triassic. We now evaluate the unaysaurid sauropodomorph Macrocollum itaquii (MÜLLER; LANGER; DIAS-DA-SILVA, 2018), the oldest and largest long-necked sauropodomorph of the lower Norian Candelária Sequence in South Brazil (MÜLLER; LANGER; DIAS-DA-SILVA, 2018). The micro-computed tomography of the skeleton of Macrocollum here presented brings novel insights into the gradual evolution of the Respiratory System in dinosaurs.

MATERIALS AND METHOD

Institutional abbreviations: CAPPA/UFSM, Centro de Apoio à Pesquisa Paleontológica da Quarta Colônia, Universidade Federal de Santa Maria, São João do Polêsine, Rio Grande do Sul, Brazil; **PVL**, Paleovertebrate collection, Instituto "Miguel Lillo", San Miguel de Tucumán, Salta, Argentina; **NHM**, Natural History Museum, London, United Kingdom; **ULBRA**, Centro de Apoio à Pesquisa Paleontológica da Quarta Colônia, Universidade Federal de Santa Maria, São João do Polêsine, Rio Grande do Sul, Brazil (previously Museu de Ciências Naturais, Universidade Luterana do Brasil, Canoas, Brazil).

Specimen

The studied specimen corresponds to a paratype of *Macrocollum itaquii* (CAPPA/UFSM 0001b), an almost complete articulated skeleton of an unaysaurid sauropodomorph (MÜLLER; LANGER; DIAS-DA-SILVA, 2018). This specimen was found associated with two other skeletons (holotype and paratype) resulting in the oldest evidence of gregarious behavior in dinosaurs. There are yet no histological thin sections to address the skeletochronology of this specimen, but the scapula and the coracoid are partially unfused. Some vertebrae present fused neurocentral sutures to a varied degree along the column, and some neural arches remain not entirely merged, which suggests a subadult ontogenetic stage (BROCHU, 1996; MÜLLER et al., 2015).

Locality and horizon

Macrocollum specimens were excavated at the Wachholz Site (29º36'46.42" S; 53º15'54.06" W), Agudo municipality, Rio Grande do Sul state, South Brazil (MÜLLER et al., 2015). This site is part of the Upper Triassic (lower Norian) Candelária Sequence, Paraná Basin. Chronocorrelated strata were dated at 225.42 ± 0.37 Ma (LANGER; RAMEZANI; DA ROSA, 2018).

Taphonomic remarks

The CAPPA/UFSM 0001 series of specimens were moderately affected by taphonomic compression, showing both subtle diagenetic distortions and cracks (MÜLLER et al., 2018). However, the external overall morphology is well preserved, except for smaller foramina as it will be further explained in the results section.

Anatomical nomenclature and terminology

We apply Wilson's terms to describe vertebral laminae, fossae, and their landmarks (WILSON, 1999, 2012; WILSON et al., 2011), Wedel's for vertebral pneumaticity (WEDEL, 2003, 2007; WEDEL; CIFELLI; SANDERS, 2000), and O'Connor's method to evaluate unambiguous PSP (O'CONNOR, 2006).

Microtomography (μCT scan)

A posterior (8th) cervical vertebra and an anterior (2nd) dorsal vertebra of *Macrocollum* were scanned in a Bruker-Skyscan 1173 microtomographer (130 kV μ-focus X-ray source; voxel size = 0.15 mm). This μCT scanner is located at the Instituto do Petróleo e dos Recursos Naturais, Universidade Católica do Rio Grande do Sul/PUCRS), Porto Alegre, Brazil. We used the open- source software 3D-Slicer v5.2 (FEDOROV et al., 2012) and CloudCompare v2.12.4 (CLOUDCOMPARE, 2018) to process the data, to generate 3D reconstructions, and to apply density-based color grades based on bone tissues (AURELIANO et al., 2020). ImageJ v1.52 (SCHNEIDER; RASBAND; ELICEIRI, 2012) was used for digital measurements. All microtomography data was uploaded to the Morphobank platform and is available through this link: http://morphobank.org/permalink/?P4526.

RESULTS

We analyzed the variation of the postcranial skeletal pneumaticity of the sauropodomorph *Macrocollum itaquii* with macroscopic inspection and computed tomography (Fig.1). Diagenetic artifacts compromised the vertebral bone tissue moderately with cracks and mineral infills, and morphology was altered to a little extent. This condition made it difficult to detect smaller nutritional foramina but, fortunately, did not affect the preservation of the larger pneumatic ones. It was possible to detect evidence of unambiguous PSP, which varies along the axial skeleton. Only presacral vertebrae demonstrated the presence of pneumatic foramina. The μCT scan of the posterior cervical element (Fig. 2) revealed that the centrum comprises mostly dense trabecular bone except for a narrow longitudinally-elongated chamber connecting with two lateral pneumatopores. There is also a decrease in trabecular density in the neural arch. Several fossae (spof, cpof and cdf) connect with internal pneumatic chambers. These chambers are neither camerate nor camellate, but a new type of tissue with an intermediate texture. We propose the term 'protocamerate chambers' (ptc) for these structures which are not large enough to be considered camerae, but also present a camellate array internally. The μCT scan of the anterior dorsal vertebra (Fig. 3), on the other hand, shows only chaotic apneumatic trabeculae in the centrum with no lateral pneumatopores. Only the neural arch is pneumatized, encompassing well-defined laminae connecting with the internal protocamerate tissue (ptc) throughout the fossae (cdf, pocdf, and prcdf). The protocamerate tissue also expands ventrodorsally to the interior base of the spinal arch.

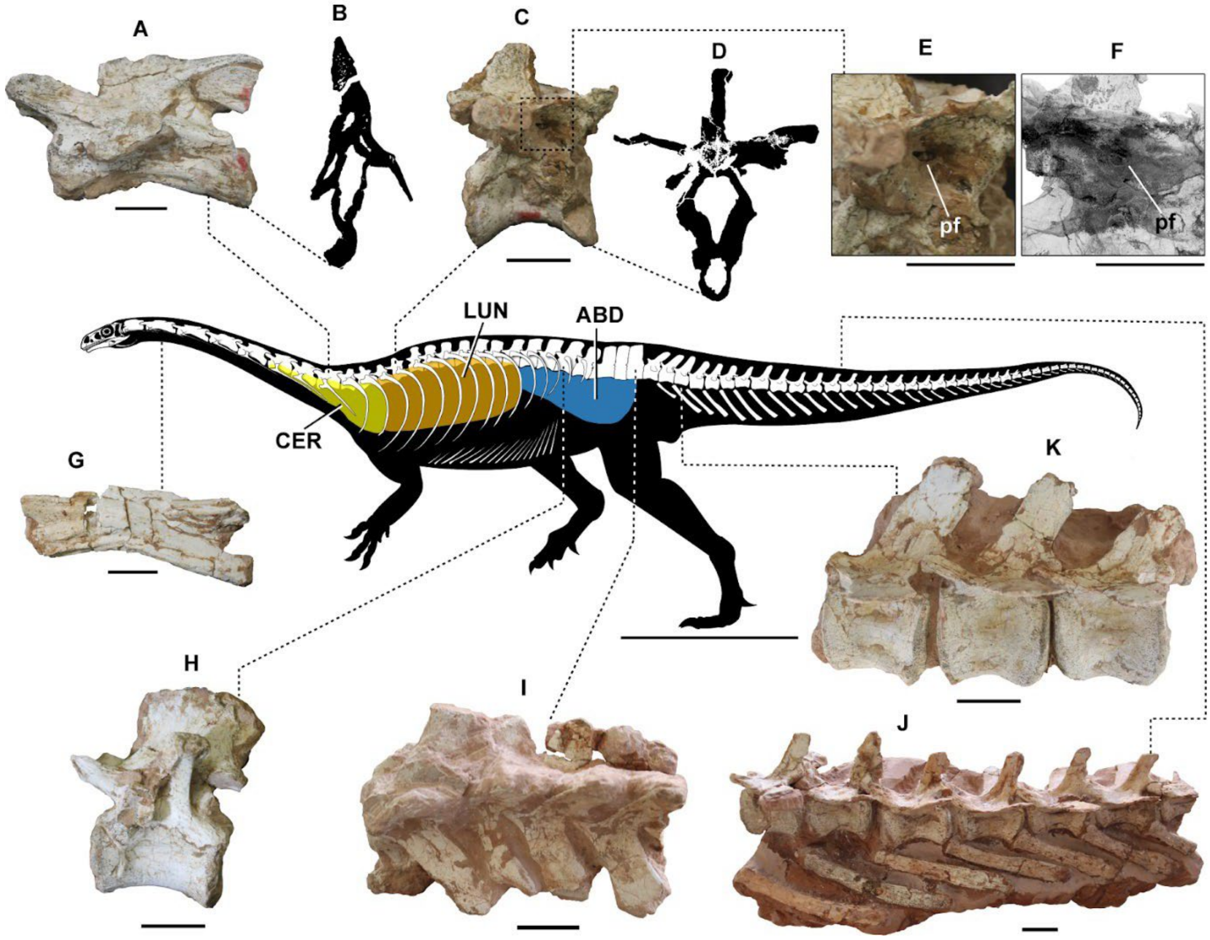

Figure 1. Skeletal reconstruction of the unaysaurid sauropodomorph *Macrocollum* (CAPPA/UFSM 0001b) showing vertebral elements along the spine and putative reconstruction of the air sac systems involved. **A**, pneumatic posterior cervical vertebra and a cross-section CT slice in **B**. **C**, a pneumatized anterior dorsal vertebra with cross-section CT slice in **D**, and detail of the pneumatic foramen in **E**. **F**, detail of the pneumatic foramen in a reconstructed 3D model of the element. **G**, anterior cervical element (apneumatic). **H**, posterior dorsal vertebra shows no traces of PSP. The sacral series (**I**), as well as the anterior (**K**) and mid-caudal (**J**) series are apneumatic. **A**, **G**, **H**, **J**, and **K** are in left lateral view. **C**, **E** and **F** are in right lateral view. **I** is in dorsal view. **Abbreviations**: **ABD**, abdominal diverticula; **CER**, cervical diverticula; **LUN**, lung; **pf**, pneumatic foramen. The reconstruction was made by Rodrigo T. Müller. Scale bar of the skeletal reconstruction = 500 mm; A-J = 20 mm.

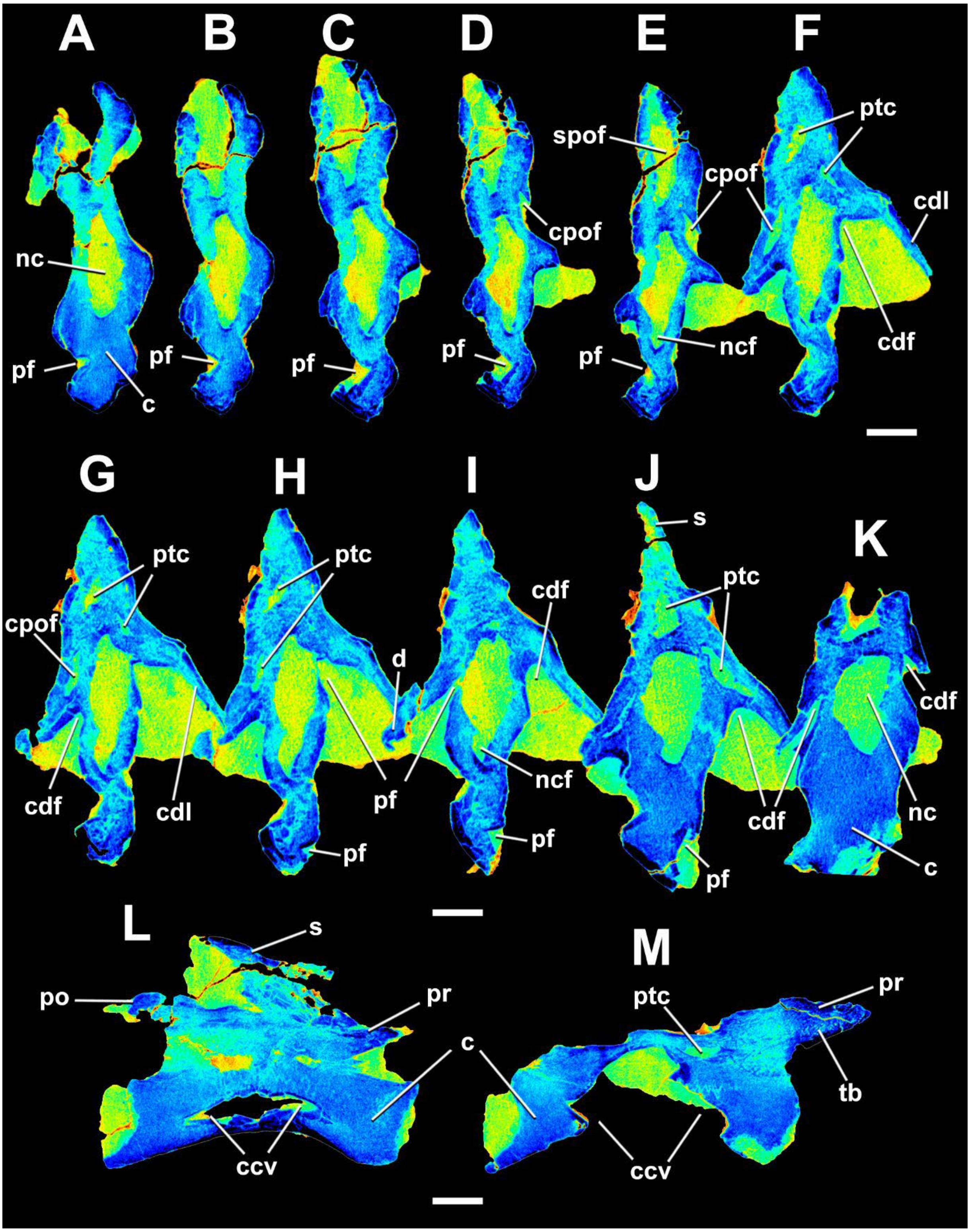

Figure 2. Micro-CT scan of the posterior (8th) cervical vertebra of the unaysaurid sauropodomorph *Macrocollum* (CAPPA/UFSM 0001b) in cross-section (**A**-**K**) and lateral views (**L**, **M**). **A** to **K** presents a cross-section series from posterior to anterior-most positions, respectively. **L** and **M** show a narrow longitudinally-elongated chamber in the centrum and a decrease in trabecular density in the prezygapophysis and the neural spine. **Abbreviations: c**, centrum; **ccv**, a chamber in the centrum; **cdf**, centrodiapophyseal fossa; **cdl,** centrodiapophyseal lamina; **cpof**, centropostzygapophyseal fossa; **d**, diapophysis; **nc**, neural canal; **ncf**, neural canal foramen; pf, pneumatic foramen; **po**, postzygapophysis; **pocdf**, postzygacentrodiapophyseal fossa; **pr**, prezygapophysis; **prcdf**, prezygacentrodiapophyseal fossa; **ptc**, protocamera; **s**, neural spine/ spof, spinopostzygapophyseal fossa. Scale bar = 10 mm.

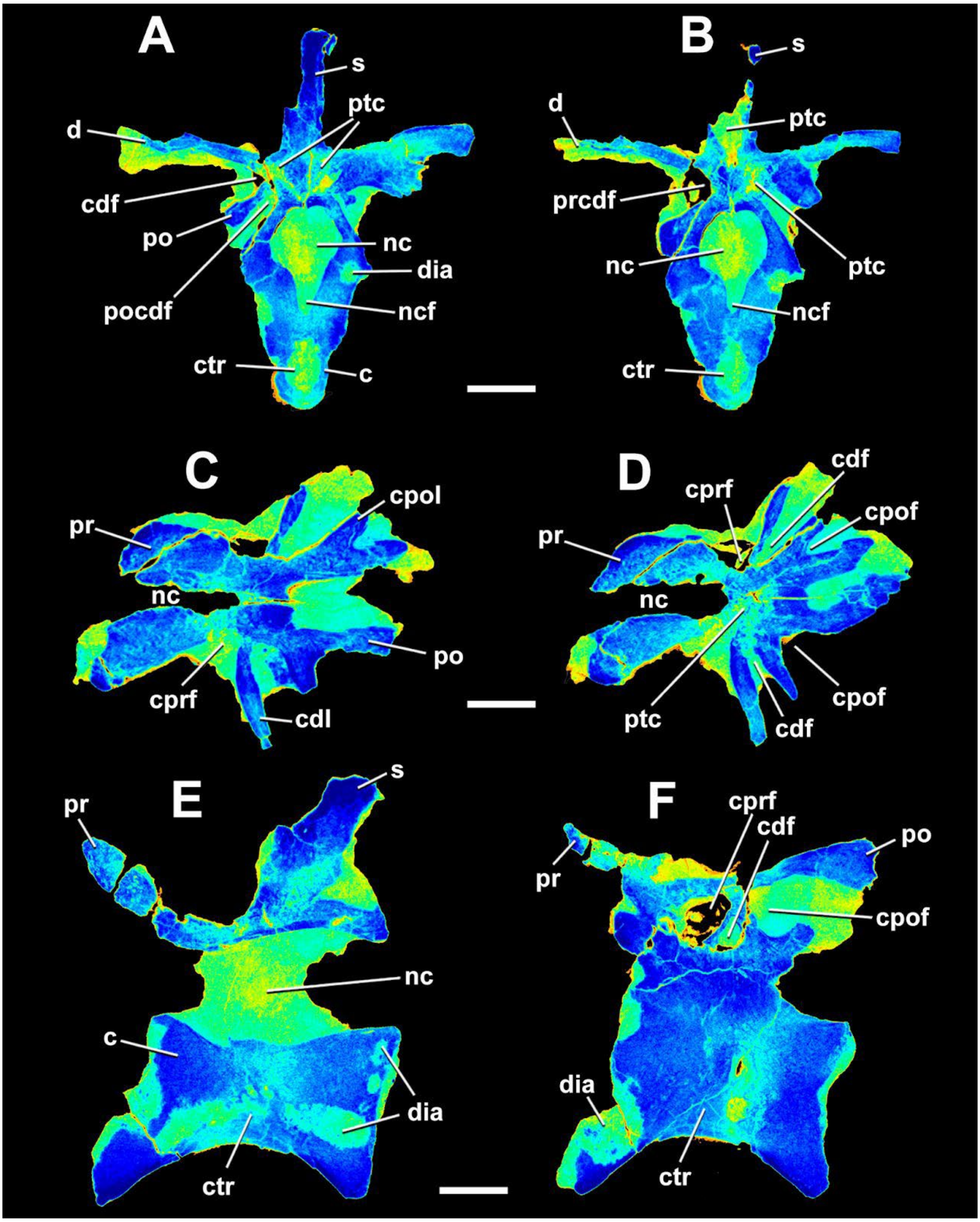

Figure 3. Micro-CT scan of the anterior (2nd) dorsal vertebra of the unaysaurid sauropodomorph Macrocollum (CAPPA/UFSM 0001b). A and B show cross-sections of the entire vertebra in anterior view at the approximate midpoint. E and F show midshaft slices in lateral view. F shows three fossae in the neural arch (cprf, cdf and cpof). Abbreviations: c, centrum; cdf, centrodiapophyseal fossa; cdl, centrodiapophyseal lamina; ctr, chaotic trabeculae; cpof, centropostzygapophyseal fossa; cpol, centropostzygapophyseal lamina; cprf, centroprezygapophyseal fossa; d, diapophysis; dia, diagenetic artifact; nc, neural canal; ncf, neural canal foramen; pf, pneumatic foramen; po, postzygapophysis; pocdf,

postzygapophysealcentrodiapophyseal fossa; pr, prezygapophysis; prcdf, prezygapophysealcentrodiapophyseal fossa; ptc, protocamera; s, neural spine. Scale bar = 10 mm.

DISCUSSION

An evaluation of the herrerasaurid Gnathovorax, and the early sauropodomorphs Buriolestes and Pampadromaeus found evidence suggesting the absence of PSP in early saurischians during the Carnian (AURELIANO et al., 2022). We now analyzed the unaysaurid *Macrocollum* from the early Norian of South Brazil. The presence of well-developed fossae communicating with internal chambers throughout foramina is the definitive evidence of unambiguous PSP (O'CONNOR, 2006). Consequently, this find represents the oldest evidence of an invasive air sac system in Sauropodomorpha.

Patterns of pneumatization in Rhaetian and Early Jurassic sauropodomorphs found PSP to be restricted to the posterior dorsal elements as in *Eucnemesaurus*, *Aardonyx*, and *Antenonitrus* (YATES; WEDEL; BONNAN, 2012). This evidence led the authors to suggest that the pneumatization process in early forms was influenced directly and solely by the abdominal air sac system, a term defined in previous studies on extant birds (MCLELLAND, 1989). According to their hypothesis, only in eusauropods would the cervical air sac system develop with phyletic consistency, and not sporadic as in non-gravisaurian taxa. The presence of pneumatopores invading the centrum in a posterior cervical vertebra and not in an anterior dorsal element in *Macrocollum* is intriguing and so far unique in early sauropodomorphs (see Table 1). The neural arches of *Macrocollum* also showed many connections between the interior pneumatic architecture and the outer fossae (cdf, cprf, cpof; see Fig.2, 3). Some *Plateosaurus* specimens also showed limited and restricted cervical pneumatization (e.g., AMNH 6810) and were considered exceptions in the evolution of the group (YATES; WEDEL; BONNAN, 2012). *Pantydraco* could potentially be another exception (YATES; WEDEL; BONNAN, 2012) but the absence of almost the entire sacral and dorsal series turns this into an unsolvable case at this point.

The presence of both cervical and dorsal pneumatization in *Macrocollum* is unique within non-gravisaurians, and could suggest the influence of both cervical and lung air sac systems invading the vertebral series. However, the absence of pneumatopores in the dorsal centra might be indicative that lung and abdominal diverticula were not invading the skeleton. The absence of evidence of PSP in posterior dorsal elements in chronologically and phylogenetically earlier forms prior to *Eucnemesaurus* contrasts with the pattern of pneumatization observed in later forms, specially anchisaurians (see Table 1 and Fig. 4). The evidence of unambiguous PSP in *Macrocollum*, *Pantydraco*, and *Plateosaurus*, when compared with the apneumatic skeleton of *Buriolestes*, *Pampadromaeus*, *Thecodontosaurus*, *Efraasia*, and *Massospondylus*, demonstrates that the initial evolution of diverticular ventilation systems followed no pattern.

Macrocollum also presented a new type of pneumatic tissue, showing properties of both camarae and camellae as defined by WEDEL (2000). We named this tissue 'protocamerae' (see ptc in Fig.2,3). This evidence supports a previous hypothesis from AURELIANO et al. (2022) in which the pneumatic tissues would not have evolved as camarae in the Jurassic and then camellae in the Cretaceous but actually derived from delicate camellate-like trabeculae. The structural change from the apneumatic pseudo-polycamerate tissue in *Pampadromaeus* during the Carnian (AURELIANO et al., 2022) to the protocamerae in *Macrocollum* is evidence of the emergence of PSP in Sauropodomorpha. Additionally, YATES et al. (2012) observed that the pneumatization throughout the infradiapophyseal fossae appears later in neosauropods due to the presence of camellate tissue, which would increase the volume and the rigidity of the neural arch, allowing the invasion of the diverticula. The invasion of air sacs throughout the cdf, cprf and cpof in *Macrocollum* could have been possible by the presence of this protocamerate tissue, with a similar structural consequence.

Table 1. Evaluation of postcranial skeletal pneumaticity in sauropodomorphs and the herrerasaurid *Gnathovorax*. Question marks indicate unknown information and/or elements.

Taxon/Specimen	Age	Anterior cervical	Posterior cervical	Anterior dorsal	Posterior dorsal	Sacral	Anterior caudal	Reference
Gnathovorax (CAPPA/UFSM 0009)	Carnian	No	No	No	No	No	No	Aureliano et al. (2022)
Buriolestes (CAPPA/UFSM 0035)	Carnian	No	No	No	No	No	No	Aureliano et al. (2022)
Pampadromaeus (ULBRAPV016)	Carnian	?	?	No	?	?	?	Aureliano et al. (2022)
Macrocollum (CAPPA/UFSM 0001b)	early Norian	No	Yes	Yes	No	No	No	This work
Plateosaurus (AMNH 6810)	late Norian - Rhaetian	No	Yes	No	No	No	No	Yates et al. (2012)
Eucnemesaurus (BP/1/6107)	late Norian - Rhaetian	?	?	?	Yes	?	?	Yates et al. (2012)
Aardonyx (BP/1/6566)	Hettangian	No	No	No	Yes	Yes	No	Yates et al. (2012)
Antenonitrus (BP/1/4952)	Sinemurian - Pliensbachian	?	?	No	Yes	?	No	Yates et al. (2012)
Haplocanthosaurus (CM879)	Kimmeridgian	Yes	Yes	Yes	Yes	Yes	Yes	Wedel (2009)
Saltasaurus (PVL 4017-214, 47, 192)	Maastrichtian	Yes	Yes	Yes	Yes	Yes	Yes	Cerda et al. (2012)b; Zurriaguz & Powell (2015)

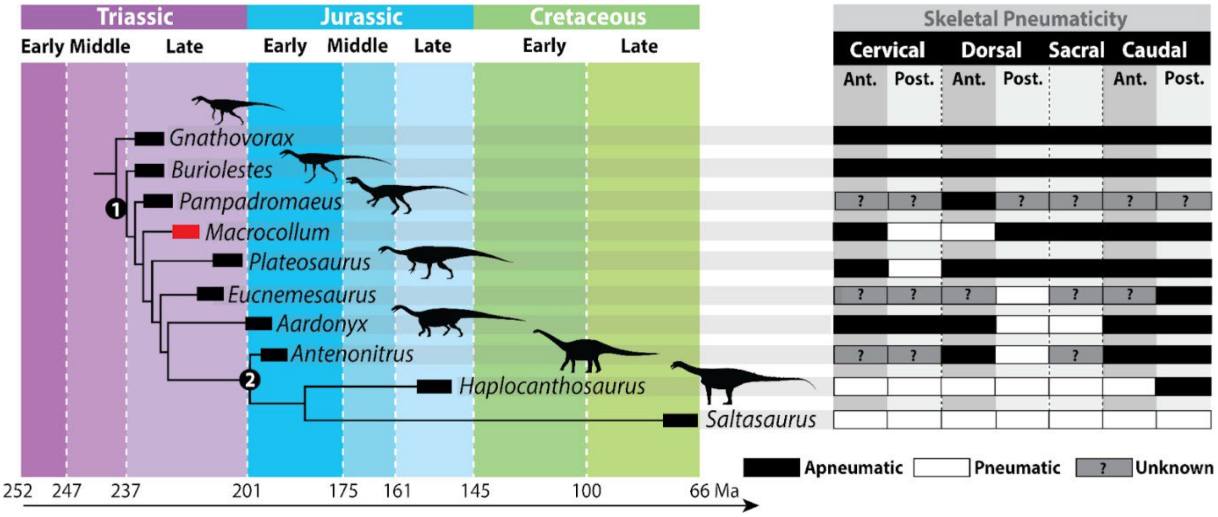

Figure 4. Chronological and phylogenetic evolution of postcranial skeletal pneumaticity in sauropodomorph dinosaurs, and the herrerasaurid *Gnathovorax* as an outgroup. **1**, Sauropodomorpha. **2**,

Sauropoda. Based on the topology by YATES et al. (2012) and MÜLLER et al. (2018b). Silhouettes are from Phylopic.org by Bruno Navarro, Mathew Wedel, Ryan Soledade, and Scott Hartman.

CONCLUSIONS

The evidence of unambiguous postcranial pneumaticity in the unaysaurid *Macrocollum itaquii* from the early Norian of Southern Brazil fetched several insights into the evolution of the air sac systems. Some of the highlights are listed below:

- The chronologically oldest and phylogenetically earliest evidence described to date of an invasive air sac system in a dinosaur.

- The pattern of pneumatization in posterior cervical and anterior dorsal vertebrae is unique in non-sauropod sauropodomorphs. Our data support the previous hypothesis showing that this clade did not develop a consistent and extensive pattern of PSP until the evolution of eusauropods in the Jurassic.

- We described a new type of pneumatic tissue, the protocamerae, showing properties of both camellate and camerate tissues found later in the Mesozoic. This changes the previous hypothesis which stated that the pneumatization of the skeleton first evolved into camarae, and only later derived into delicate trabecular camellae. The protocamerate tissue is evidence of delicate thin tissue forming larger chambers.

Macrocollum is an example of gradual evolution of both morphology and histology, with the skeletal tissues adapting to the invasion of the air sac diverticula. We suggest that the great number of new taxa and specimens of Late Triassic sauropodomorphs described in the recent decade should be also sampled since they have the potential to provide a high-resolution understanding of the evolution of the Respiratory System in dinosaurs. Finally, the usage of microtomography coupled with histological thin sections should be encouraged in future approaches to achieve this goal.

ACKNOWLEDGEMENTS

We thank Adolpho Herbert Augustin for conducting the microtomography. We also would like to thank Pedro Buck, Felipe Pinheiro, Ariel Martine, Giorgio Basilici, Blair McPhee, and Ignacio Cerda for their comments on an earlier version of this article. Research grants, scholarships, and financial aid were provided by Fundação de Amparo à Pesquisa do Estado de São Paulo (FAPESP 2019/16727-3) 'Taphonomical landscapes' (F.R.B.), Fundação de Amparo à Pesquisa do Estado do Rio Grande do Sul (FAPERGS 1/2551-0002030-0, L.K.; 21/2551-0000680-3, R.T.M.), and Conselho Nacional de Desenvolvimento Científico e Tecnológico (CNPq grant 307333/2021-3, F.R.B.; CNPq 404095/2021-6. R.T.M.; 422568/2018-0; 309414/2019-9, L.K.).

Bibliography

3 Discussão

Além do que já foi discutido dentro de cada artigo resultante deste projeto de doutorado, existem algumas observações que permeiam ambos manuscritos.

A microtomografia computadorizada continua sendo uma técnica essencial para um diagnóstico de PSP não-ambíguo. Mesmo em espécimes parcialmente comprometidos pela diagênese, alguns resquícios das trabéculas e câmaras originais podem se preservar. Artefatos podem dificultar a identificar a arquitetura, mas o auxílio de falsa-cor facilita este trabalho, possibilidade reverter dificuldades que alguns colegas tiveram no passado (BUTLER; BARRETT; GOWER, 2012).

Os resultados obtidos a partir das análises dos dinossauros saurísquios do Carniano e Noriano da Bacia do Paraná se complementam, por mostrarem o ponto cronológico e filogenético de pelo menos uma das origens dos sacos aéreos. Não obstante, os próximos passos consistiriam em investigar a evolução dos terópodes e pterossauromorfos, replicando os métodos desenvolvidos nesta tese. Os fósseis do Brasil demonstram um potencial para ampliar em muito a resolução do conhecimento da evolução do Sistema Respiratório nos avemetatarsálios.

Na vertente das lâminas histológicas, demonstrou-se muito útil trazer conceitos da mineralogia ótica como relevo ótico, extinção, birrefringência e textura. Como os diferentes tipos de fibras ósseas (Sharpey, pneumósteo e lamelar) são semelhantes quando observadas superficialmente, as novas propriedades redefinem a maneira como poderão ser detectados tais tecidos em trabalhos futuros. Uma continuidade desta linha seria testar se as mesmas propriedades se aplicam em tecido ósseo de animais viventes, uma vez que seja esperado, pois a estrutura principal da hidroxiapatita deveria se conservar indefinidamente.

4 Conclusão

Os resultados oriundos desta tese de doutorado demonstraram alto impacto dentro dos objetivos propostos. Por um lado, houve contribuição para um antigo enigma quanto às origens dos sacos aéreos em avemetatarsálios. Adicionalmente, contribuiu-se para uma melhor definição do pneumósteo, trazendo conceitos de petrografia e mineralogia ótica para a histologia. A replicação dos métodos aqui aprimorados poderá auxiliar colegas na ampliação do conhecimento sobre a evolução do Sistema Respiratório em dinossauros e outros avemetatarsálios, bem como auxiliar na descrição da microanatomia de uma grande variedade de organismos.

5 Referências Bibliográficas

ARANCIAGA ROLANDO, M.; GARCIA MARSÀ, J.; NOVAS, F. Histology and pneumaticity of *Aoniraptor libertatem* (Dinosauria, Theropoda), an enigmatic mid-sized megaraptoran from Patagonia. **Journal of anatomy**, v. 237, n. 4, p. 741–756, Oct. 2020.

AURELIANO, T. et al. On the occurrence of Pterosauria in Exu, Pernambuco (Lower Cretaceous Romualdo Formation, Araripe Basin), Northeastern Brazil. **Estudos Geológicos**, v. 24, n. 2, p. 15–27, 2014.

AURELIANO, T. et al. Semi-aquatic adaptations in a spinosaur from the Lower Cretaceous of Brazil. **Cretaceous Research**, v. 90, p. 283–295, 2018.

AURELIANO, T. et al. Influence of taphonomy on histological evidence for vertebral pneumaticity in an Upper Cretaceous titanosaur from South America. **Cretaceous Research**, v. 108, p. 104337, 1 Apr. 2020. 2020.

AURELIANO, T. et al. Blood parasites and acute osteomyelitis in a non-avian dinosaur (Sauropoda, Titanosauria) from the Upper Cretaceous Adamantina Formation, Bauru basin, Southeast Brazil. **Cretaceous Research**, v. 118, p. 104672, 2021a.

AURELIANO, T. et al. Exquisite air sac histological traces in a hyperpneumatized nanoid sauropod dinosaur from South America. **Scientific reports**, v. 11, n. 1, p. 24207, 17 Dec. 2021b.

AURELIANO, T. et al. The absence of an invasive air sac system in the earliest dinosaurs suggests multiple origins of vertebral pneumaticity. **Scientific reports**, v. 12, n. 1, p. 20844, 9 Dec. 2022.

BAILLEUL, A. M. et al. Evidence of proteins, chromosomes and chemical markers of DNA in exceptionally preserved dinosaur cartilage. **National science review**, v. 7, n. 4, p. 815–822, Apr. 2020.

BENSON, R. B. J. et al. Air-filled postcranial bones in theropod dinosaurs: physiological implications and the ’reptile’-bird transition. **Biological reviews of the Cambridge Philosophical Society**, v. 87, n. 1, p. 168–193, Feb. 2012.

BREMER. The Pneumatization of the Humerus in Common Fowl and the Associated Activity of Theelin. **The Anatomical record**, 1940.

BRITT, B. B. Pneumatic postcranial bones in dinosaurs and other archosaurs. 1994.

BRITT, B. B. et al. Postcranial pneumatization in Archaeopteryx. **Nature**, v. 395, n. 6700, p. 374–376, Sep. 1998.

BRUM, A. S. et al. Description of uncommon pneumatic structures of a noasaurid (Theropoda, Dinosauria) cervical vertebra from the Bauru Group (Upper Cretaceous), Brazil. **Cretaceous Research**, v. 85, p. 193–206, 1 May 2018.

BRUM, A. S. et al. Microstructure of axial bones of lithostrotian titanosaurs (Neosauropoda: Sauropodomorpha) shows extended fast-growing phase. **Cretaceous Research**, v. 136, p. 105220, 1 Aug. 2022.

BRUSATTE, S. L.; O’CONNOR, J. K.; JARVIS, E. D. The Origin and Diversification of Birds. **Current biology: CB**, v. 25, n. 19, p. R888-98, 5 Oct. 2015.

BUCHMANN, R.; RODRIGUES, T. The Evolution of Pneumatic Foramina in Pterosaur Vertebrae. **Anais da Academia Brasileira de Ciencias**, v. 91Suppl. 2, n. Suppl. 2, p. e20180782, 6 May 2019.

BUFFRÉNIL, V. et al. **Vertebrate Skeletal Histology and Paleohistology**. [s.l.] CRC Press, 2021.

BUTLER, R. J.; BARRETT, P. M.; GOWER, D. J. Postcranial skeletal pneumaticity and air-sacs in the earliest pterosaurs. **Biology letters**, v. 5, n. 4, p. 557–560, 23 Aug. 2009.

BUTLER, R. J.; BARRETT, P. M.; GOWER, D. J. Reassessment of the evidence for postcranial skeletal pneumaticity in Triassic archosaurs, and the early evolution of the avian respiratory system. **PloS one**, v. 7, n. 3, p. e34094, 28 Mar. 2012.

CANALE, J. I. et al. Small-sized abelisaurid (Theropoda: Ceratosauria) remains from the Upper Cretaceous of northwest Patagonia, Argentina. **Cretaceous Research**, v. 62, p. 18–28, 2016.

CERDA, I. A. et al. Novel insight into the origin of the growth dynamics of sauropod dinosaurs. **PloS one**, v. 12, n. 6, p. e0179707, 27 Jun. 2017.

CERDA, I.; SALGADO, L.; POWELL, J. E. Extreme postcranial pneumaticity in sauropod dinosaurs from South America. **Paläontologische Zeitschrift**, v. 86, p. 441–449, 2012.

CHINSAMY-TURAN, A. The microstructure of dinosaur bone: deciphering biology with fine-scale techniques. 2005.

CLAESSENS, L. P. A. M.; O'CONNOR, P. M.; UNWIN, D. M. Respiratory evolution facilitated the origin of pterosaur flight and aerial gigantism. **PloS one**, v. 4, n. 2, p. e4497, 18 Feb. 2009.

CLOUDCOMPARE. Version 2.9. 1 [GPL software]. 2018.

DUMONT, M. et al. Size and size distribution of apatite crystals in sauropod fossil bones. **Palaeogeography, palaeoclimatology, palaeoecology**, v. 310, n. 1, p. 108–116, 15 Sep. 2011.

DUNCKER. The lung air sac system of birds-a contribution to the functional anatomy of the respiratory apparatus. Adu. Anat. E'mbryol. **Cell biology**, 1971.

FABBRI, M. et al. Subaqueous foraging among carnivorous dinosaurs. **Nature**, v. 603, n. 7903, p. 852–857, 23 Mar. 2022.

FEDOROV, A. et al. 3D Slicer as an image computing platform for the Quantitative Imaging Network. **Magnetic resonance imaging**, v. 30, n. 9, p. 1323–1341, Nov. 2012.

FIORILLO, A. R.; GANGLOFF, R. A. Theropod teeth from the Prince Creek Formation (Cretaceous) of northern Alaska, with speculations on Arctic dinosaur paleoecology. **Journal of Vertebrate Paleontology**, v. 20, n. 4, p. 675–682, 19 Jan. 2001.

FRANCILLON-VIEILLOT, H. et al. Microstructure and mineralization of vertebrate skeletal tissues. **Skeletal biomineralization: patterns, processes and evolutionary trends**, v. 1, p. 471–530, 1990.

FRANCILLON-VIELLOT, H. et al. **Microstructure and mineralization of vertebrate skeletal tissues. In (J. Carter, Ed.) Skeletal Biomineralization: Patterns, Processes and Evolutionary Trends, vol. 1**. New York: Van Nostrand Reinhold, , 1990.

GIANECHINI, F. A.; ZURRIAGUZ, V. L. Vertebral pneumaticity of the paravian theropod *Unenlagia comahuensis*, from the Upper Cretaceous of Patagonia, Argentina. **Cretaceous Research**, p. 104925, 11 Jun. 2021.

GODOY, P. L. Crocodylomorph cranial shape evolution and its relationship with body size and ecology. **Journal of evolutionary biology**, 18 Sep. 2019.

GOWER, D. J. Possible postcranial pneumaticity in the last common ancestor of birds and crocodilians: evidence from Erythrosuchus and other Mesozoic archosaurs. **Die Naturwissenschaften**, v. 88, n. 3, p. 119–122, Mar. 2001.

GRIFFIN, C. T. et al. Africa's oldest dinosaurs reveal early suppression of dinosaur distribution. **Nature**, v. 609, n. 7926, p. 313–319, Sep. 2022.

GRIFFIN, C. T.; NESBITT, S. J. The femoral ontogeny and long bone histology of the Middle Triassic (?late Anisian) dinosauriform *Asilisaurus kongwe* and implications for the growth of early dinosaurs. **Journal of Vertebrate Paleontology**, v. 36, n. 3, p. e1111224, 3 May 2016.

HANNA, R. R. Multiple injury and infection in a sub-adult theropod dinosaur *Allosaurus fragilis* with comparisons to allosaur pathology in the Cleveland-Lloyd Dinosaur Quarry Collection. **Journal of Vertebrate Paleontology**, v. 22, n. 1, p. 76–90, 14 Mar. 2002.

HOUSSAYE, A. "Pachyostosis" in aquatic amniotes: a review. **Integrative zoology**, v. 4, n. 4, p. 325–340, 1 Dec. 2009.

HOUSSAYE, A.; SANDER, P. M.; KLEIN, N. Adaptive Patterns in Aquatic Amniote Bone Microanatomy—More Complex than Previously Thought. **Integrative and comparative biology**, v. 56, n. 6, p. 1349–1369, 29 Oct. 2016.

HUDGINS, M. N.; UHEN, M. D.; HINNOV, L. A. The evolution of respiratory systems in Theropoda and Paracrocodylomorpha, the end-Triassic extinction, and the role of Late Triassic atmospheric O2 and CO2. **Palaeogeography, palaeoclimatology, palaeoecology**, p. 109638, 10 Feb. 2020.

HUTTENLOCKER, A. K.; WOODWARD, H. N.; HALL, B. K. The biology of bone. **Bone histology of fossil tetrapods**, p. 13–34, 2013.

IBRAHIM, N. et al. Tail-propelled aquatic locomotion in a theropod dinosaur. **Nature**, v. 581, n. 7806, p. 67–70, May 2020.

KAKEI, M. et al. High-resolution electron microscopy of the crystallites of fossil enamels obtained from various geological ages. **Journal of dental research**, v. 80, n. 6, p. 1560–1564, Jun. 2001.

KLEIN, C.; DUTROW, B. **Manual of mineral science**. [s.l.] Wiley, 2007.

KRUPANDAN, E.; CHINSAMY-TURAN, A.; POL, D. The Long Bone Histology of the Sauropodomorph, Antetonitrus ingenipes. **Anatomical record** , v. 301, n. 9, p. 1506–1518, Sep. 2018.

LAMBERTZ, M.; BERTOZZO, F.; SANDER, P. M. Bone histological correlates for air sacs and their implications for understanding the origin of the dinosaurian respiratory system. **Biology letters**, v. 14, n. 1, Jan. 2018.

LAMM, E. T. Preparation and Sectioning of Specimens. In: PADIAN, K.; LAMM, E. T. (Eds.). **Bone histology of fossil tetrapods: advancing methods, analysis, and interpretation**. California: University of California Press, 2013a. p. 55–160.

LAMM, E.-T. Preparation and Sectioning of Specimens. In: **Bone Histology of Fossil Tetrapods**. [s.l.] University of California Press, 2013b.

LAMM; PADIAN. Preparation and sectioning of specimens. **Bone histology of fossil tetrapods**, 2013.

LANGER, M. C. et al. Anatomy of the dinosaur *Pampadromaeus barberenai* (Saurischia—Sauropodomorpha) from the Late Triassic Santa Maria Formation of southern Brazil. **PloS one**, v. 14, n. 2, p. e0212543, 2019.

LANGER, M. C.; RAMEZANI, J.; DA ROSA, Á. A. S. U-Pb age constraints on dinosaur rise from south Brazil. **Gondwana Research**, v. 57, p. 133–140, 1 May 2018.

LANGER, M. C.; RIBEIRO, A. M.; SCHULTZ, C. L. The continental tetrapod-bearing Triassic of south

Brazil. **New Mexico Museum of**, 2007.

MANNING, P. L.; EGERTON, V. M.; ROMANO, M. A new sauropod dinosaur from the Middle Jurassic of the United Kingdom. **PloS one**, v. 10, n. 6, p. e0128107, 1 Jun. 2015.

MARCHETTI, I. et al. Morphological and paleohistological description of a new Baurusuchidae specimen from the Adamantina Formation, Upper Cretaceous of Brazil. **Journal of South American Earth Sciences**, v. 114, p. 103693, 1 Mar. 2022.

MENDÉZ, A. H.; NOVAS, F.; IORI, F. V. First record of Megaraptora (Theropoda, Neovenatoridae) from Brazil. **Comptes rendus. Palevol**, v. 11, p. 251–256, 2012.

MITCHELL, J.; SANDER, P. M. The three-front model: a developmental explanation of long bone diaphyseal histology of Sauropoda. **Biological journal of the Linnean Society. Linnean Society of London**, v. 112, n. 4, p. 765–781, 1 Aug. 2014.

MOORE, A. J. Vertebral pneumaticity is correlated with serial variation in vertebral shape in storks. **Journal of anatomy**, v. 238, n. 3, p. 615–625, Mar. 2021.

MÜLLER, R. T. et al. Early evolution of sauropodomorphs: anatomy and phylogenetic relationships of a remarkably well-preserved dinosaur from the Upper Triassic of southern Brazil. **Zoological journal of the Linnean Society**, v. 184, n. 4, p. 1187–1248, 7 Dec. 2018.

MÜRER, F. K. et al. 3D Maps of Mineral Composition and Hydroxyapatite Orientation in Fossil Bone Samples Obtained by X-ray Diffraction Computed Tomography. **Scientific reports**, v. 8, n. 1, p. 10052, 3 Jul. 2018.

NAVARRO, B. A. et al. A new nanoid titanosaur (Dinosauria: Sauropoda) from the Upper Cretaceous of Brazil. **Ameghiniana**, v. 59, n. 5, p. 317–354, 15 Sep. 2022.

NESBITT, S. J. The Early Evolution of Archosaurs: Relationships and the Origin of Major Clades. **Bulletin of the American Museum of Natural History**, v. 352, p. 1–292, 29 Apr. 2011.

NOVAS, F. E. et al. Review of the fossil record of early dinosaurs from South America, and its phylogenetic implications. **Journal of South American Earth Sciences**, v. 110, p. 103341, 1 Oct. 2021.

O'CONNOR, J. K.; CHIAPPE, L. M. A revision of enantiornithine (Aves: Ornithothoraces) skull morphology. **Journal of Systematic Palaeontology**, 2011.

O'CONNOR, P. M. Pulmonary pneumaticity in the postcranial skeleton of extant Aves: a case study examining Anseriformes. **Journal of morphology**, v. 261, n. 2, p. 141–161, Aug. 2004.

O'CONNOR, P. M. Postcranial pneumaticity: an evaluation of soft-tissue influences on the postcranial skeleton and the reconstruction of pulmonary anatomy in archosaurs. **Journal of morphology**, v. 267, n. 10, p. 1199–1226, 2006.

O'CONNOR, P. M. The postcranial axial skeleton of *Majungasaurus cretanissimus* (Theropoda: Abelisauridae) from the Late Cretaceous of Madagascar. **Journal of Vertebrate Paleontology**, v. 27, n. sup2, p. 127–163, 12 Jun. 2007.

PACHECO, C. et al. *Gnathovorax cabreirai*: a new early dinosaur and the origin and initial radiation of predatory dinosaurs. **PeerJ**, v. 7, p. e7963, 8 Nov. 2019.

PADIAN, K.; DE RICQLES, A. J.; HORNER, J. R. Bone histology determines identification of a new fossil taxon of pterosaur (Reptilia: Archosauria). **COMPTES RENDUS-ACADEMIE DES SCIENCES PARIS SERIE 2 SCIENCES DE LA TERRE ET DES PLANETES FASCICULE A**, v. 320, p. 77–77, 1995.

PADIAN, K.; LAMM, E.-T. **Bone Histology of Fossil Tetrapods: Advancing Methods, Analysis, and**

Interpretation. [s.l.] University of California Press, 2013.

PADIAN, K.; WOODWARD, H. N. Archosauromorpha: Avemetatarsalia – Dinosaurs and Their Relatives. In: BUFFRÉNIL, V. et al. (Eds.). **Vertebrate Skeletal Histology and Paleohistology**. [s.l.] CRC Press, 2021. p. 511–549.

PEREYRA, M. E. et al. Osteohistological correlates of muscular attachment in terrestrial and freshwater Testudines. **Journal of anatomy**, v. 234, n. 6, p. 875–898, Jun. 2019.

PERRY, S. F. et al. Implications of an avian-style respiratory system for gigantism in sauropod dinosaurs. **Journal of experimental zoology. Part A, Ecological genetics and physiology**, v. 311, n. 8, p. 600–610, 2009.

PETERMANN, H.; SANDER, M. Histological evidence for muscle insertion in extant amniote femora: implications for muscle reconstruction in fossils. **Journal of anatomy**, v. 222, n. 4, p. 419–436, Apr. 2013.

PIECHOWSKI, R.; TAŁANDA, M.; DZIK, J. Skeletal variation and ontogeny of the Late Triassic Dinosauriform *Silesaurus opolensis*. **Journal of Vertebrate Paleontology**, v. 34, n. 6, p. 1383–1393, 19 Sep. 2014.

PROCTOR, N. S.; LYNCH, P. J. **Manual of ornithology: avian structure & function**. [s.l.] Yale University Press, 1993.

RAITH, M. M.; RAASE, P. R.; REINHARDT, J. R. **Guide to thin section microscopy**. [s.l.] University of Bonn, 2011.

SALGADO, L.; CARVALHO, I. S. UBERABATITAN RIBEIROI, A NEW TITANOSAUR FROM THE MARÍLIA FORMATION (BAURU GROUP, UPPER CRETACEOUS), MINAS GERAIS, BRAZIL. **Palaeontology**, 2008.

SANCHEZ, S. et al. 3D microstructural architecture of muscle attachments in extant and fossil vertebrates revealed by synchrotron microtomography. **PloS one**, v. 8, n. 2, p. e56992, 26 Feb. 2013.

SANDER, P. M. et al. Sauropod bone histology and its implications for sauropod biology. In: KLEIN, N. et al. (Eds.). **Biology of the Sauropod Dinosaurs: Understanding the Life of Giants**. Indianapolis: Indiana University Press, 2011a. p. 276–302.

SANDER, P. M. et al. Biology of the sauropod dinosaurs: the evolution of gigantism. **Biological reviews of the Cambridge Philosophical Society**, v. 86, n. 1, p. 117–155, Feb. 2011b.

SANDER, P. M. An evolutionary cascade model for sauropod dinosaur gigantism--overview, update and tests. **PloS one**, v. 8, n. 10, p. e78573, 30 Oct. 2013.

SANTUCCI, R. M.; ARRUDA-CAMPOS, A. C. DE. A new sauropod (Macronaria, Titanosauria) from the Adamantina Formation, Bauru Group, Upper Cretaceous of Brazil and the phylogenetic relationships of Aeolosaurini. **Zootaxa**, v. 3085, p. 1–33, 2011.

SCHNEIDER, C. A.; RASBAND, W. S.; ELICEIRI, K. W. NIH Image to ImageJ: 25 years of image analysis. **Nature methods**, v. 9, n. 7, p. 671–675, Jul. 2012.

SCHWARZ, D.; FRITSCH, G. Pneumatic structures in the cervical vertebrae of the Late Jurassic Tendaguru sauropods *Brachiosaurus brancai* and *Dicraeosaurus*. **Eclogae Geologicae Helvetiae**, v. 99, n. 1, p. 65–78, 1 May 2006.

SILVA JUNIOR, J. C. G. et al. Osteology and systematics of Uberabatitan ribeiroi (Dinosauria; Sauropoda): a Late Cretaceous titanosaur from Minas Gerais, Brazil. **Zootaxa**, v. 4577, n. 3, p. 401–438, 2019.

SILVA JUNIOR, J. C. G. et al. Reassessment of *Aeolosaurus maximus*, a titanosaur dinosaur from the Late Cretaceous of Southeastern Brazil. **Historical biology**, v. 34, n. 3, p. 403–411, 4 Mar. 2022.

SMUTS, M. M. The venous drainage of the cervical vertebrae of the ox (Bos taurus L.). **The Onderstepoort journal of veterinary research**, v. 44, n. 4, p. 233–247, Dec. 1977.

SOUZA, G. A. et al. The first edentulous ceratosaur from South America. **Scientific reports**, v. 11, n. 1, p. 22281, 18 Nov. 2021a.

SOUZA, L. G. D. E. et al. The history, importance and anatomy of the specimen that validated the giant *Purussaurus brasiliensis* Barbosa-Rodrigues 1892 (Crocodylia: Caimaninae). **Anais da Academia Brasileira de Ciencias**, v. 93, n. suppl 2, p. e20200369, 16 Jun. 2021b.

STEIN, K.; SANDER, P. M. **Histological core drilling: a less destructive method for studying bone histology**. Methods in fossil preparation: proceedings of the first annual Fossil Preparation and Collections Symposium. **Anais**...ebook]: Petrified Forest National Park, 2009.

TAYLOR, M.; WEDEL, M. Why is vertebral pneumaticity in sauropod dinosaurs so variable? **Qeios**, 20 Jan. 2021.

TRUEMAN, C. N.; TUROSS, N. Trace Elements in Recent and Fossil Bone Apatite. **Reviews in Mineralogy and Geochemistry**, v. 48, n. 1, p. 489–521, 1 Jan. 2002.

WEDEL, M. J. Vertebral pneumaticity, air sacs, and the physiology of sauropod dinosaurs. **Paleobiology**, v. 29, n. 2, p. 243–255, 2003a.

WEDEL, M. J. The evolution of vertebral pneumaticity in sauropod dinosaurs. **Journal of Vertebrate Paleontology**, v. 23, n. 2, p. 344–357, 17 Jun. 2003b.

WEDEL, M. J. Origin of postcranial skeletal pneumaticity in dinosaurs. **Integrative zoology**, v. 1, n. 2, p. 80–85, Jun. 2006.

WEDEL, M. J. What pneumaticity tells us about ‘prosauropods’, and vice versa. **Special Papers in Palaeontology**, v. 77, p. 207–222, 2007.

WEDEL, M. J. Evidence for bird-like air sacs in saurischian dinosaurs. **Journal of experimental zoology. Part A, Ecological genetics and physiology**, v. 311, n. 8, p. 611–628, 2009.

WEDEL, M. J.; CIFELLI, R. L.; SANDERS, R. K. Osteology, paleobiology, and relationships of the sauropod dinosaur *Sauroposeidon*. **Acta palaeontologica Polonica**, v. 45, p. 343–388, 2000.

WEDEL, M. J.; TAYLOR, M. P. Caudal pneumaticity and pneumatic hiatuses in the sauropod dinosaurs Giraffatitan and Apatosaurus. **PloS one**, v. 8, n. 10, p. e78213, 30 Oct. 2013.

WILLIAMS, C. J. et al. Helically arranged cross struts in azhdarchid pterosaur cervical vertebrae and their biomechanical implications. **iScience**, v. 24, n. 4, p. 102338, 23 Apr. 2021.

WILSON, J. A. A nomenclature for vertebral laminae in sauropods and other saurischian dinosaurs. **Journal of Vertebrate Paleontology**, v. 19, n. 4, p. 639–653, 13 Dec. 1999.

WILSON, J. A. et al. A nomenclature for vertebral fossae in sauropods and other saurischian dinosaurs. **PloS one**, v. 6, n. 2, p. e17114, 28 Feb. 2011.

WILSON, J. A. New vertebral laminae and patterns of serial variation in vertebral laminae of sauropod dinosaurs. 2012.

WOODRUFF, D. C. et al. The first occurrence of an avian-style respiratory infection in a non-avian dinosaur. **Scientific reports**, v. 12, n. 1, p. 1954, 10 Feb. 2022.

WOODWARD, H. N.; LEHMAN, T. M. Bone histology and microanatomy of *Alamosaurus sanjuanensis* (Sauropoda: Titanosauria) from the Maastrichtian of Big Bend National Park, Texas. **Journal of Vertebrate Paleontology**, v. 29, n. 3, p. 807–821, 12 Sep. 2009.

YATES, A. M.; WEDEL, M. J.; BONNAN, M. F. The Early Evolution of Postcranial Skeletal Pneumaticity in Sauropodomorph Dinosaurs. **Acta Palaeontologica Polonica**, v. 57, n. 1, p. 85–100, Mar. 2012.

Anexo

Autorização da Editora Nature para inclusão do conteúdo do artigo 1 desta tese no corpo do texto da mesma

Open Access This article is licensed under a Creative Commons Attribution 4.0 International License, which permits use, sharing, adaptation, distribution and reproduction in any medium or format, as long as you give appropriate credit to the original author(s) and the source, provide a link to the Creative Commons licence, and indicate if changes were made. The images or other third party material in this article are included in the article's Creative Commons licence, unless indicated otherwise in a credit line to the material. If material is not included in the article's Creative Commons licence and your intended use is not permitted by statutory regulation or exceeds the permitted use, you will need to obtain permission directly from the copyright holder. To view a copy of this licence, visit http://creativecommons.org/licenses/by/4.0/.